Evaluation of Reanalysis Estimates of Precipitation, Radiation, and Temperature over Benin (West Africa)

RENÉ BODJRENOU,[a,b,e] JEAN-MARTIAL COHARD,[b] BASILE HECTOR,[b] EMMANUEL AGNIDÉ LAWIN,[a] GUILLAUME CHAGNAUD,[b] DERRICK KWADWO DANSO,[c] YEKAMBESSOUN N'TCHA M'PO,[a] FÉLICIEN BADOU,[d] AND BERNARD AHAMIDE[e]

[a] *Laboratory of Applied Hydrology, National Water Institute, University of Abomey-Calavi, Abomey-Calavi, Benin*
[b] *Institute of Engineering and Management, University of Grenoble Alpes, CNRS, IRD, IGE, Grenoble, France*
[c] *Department of Geological and Atmospheric Sciences, Iowa State University, Ames, Iowa*
[d] *National University of Agriculture, Ketou, Benin*
[e] *Faculty of Agricultural Sciences, University of Abomey-Calavi, Abomey-Calavi, Benin*

(Manuscript received 13 October 2021, in final form 8 July 2023, accepted 18 July 2023)

ABSTRACT: In West Africa, climatic data issues, especially availability and quality, remain a significant constraint to the development and application of distributed hydrological modeling. As alternatives to ground-based observations, reanalysis products have received increasing attention in recent years. This study aims to evaluate three reanalysis products, namely, ERA5, Water and Global Change (WATCH) Forcing Data (WFD) ERA5 (WFDE5), and MERRA-2, from 1981 to 2019 to determine their ability to represent four hydrological climates variables over a range of space and time scales in Benin. The variables from the reanalysis products are compared with point station databased metrics Kling–Gupta efficiency (KGE), mean absolute error (MAE), correlation, and relative error in precipitation annual (REPA). The results show that ERA5 presents a better correlation for annual mean temperature (between 0.74 and 0.90) than do WFDE5 (0.63–0.78) and MERRA-2 (0.25–0.65). Both ERA5 and WFDE5 are able to reproduce the observed upward trend of temperature (0.2°C decade^{-1}) in the region. We noted a systematic cold bias of ~1.3°C in all reanalyses except WFDE5 (~0.1°C). On the monthly time scale, the temperature of the region is better reproduced by ERA5 and WFDE5 (KGE $\geq$ 0.80) than by MERRA-2 (KGE $<$ 0.5). At all time scales, WFDE5 produces the best MAE scores for longwave (LW) and shortwave (SW) radiation, followed by ERA5. WFDE5 also provides the best estimates for the annual precipitation (REPA $\in$]−25, 25[and KGE $\geq$ 50% at most stations). ERA5 produces similar results, but MERRA-2 performs poorly in all the metrics. In addition, ERA5 and WFDE5 reproduce the bimodal rainfall regime in southern Benin, unlike MERRA-2, but all products have too many small rainfall events.

KEYWORDS: Africa; Climate change; Climate variability; Hydrometeorology; Longwave radiation; Temperature

1. Introduction

Hydrological studies remain essential to understanding the effects of climate change on water resources. Hydrological models (global, distributed, and semidistributed) are the standard tools for that purpose, and their performance is highly dependent on the quality of the required meteorological and vegetation forcing fields (Clark et al. 2009; Ocio et al. 2019). In regions like West Africa, data gaps caused by low-density station networks, discontinuous monitoring, limited personnel, power shortages, and long sensor replacement periods have hindered attempts to document the water cycle evolution. These irregularities initially drove the development of spatialization and interpolation techniques, each of which has its limitations (Ly et al. 2013). The uncertainties in measuring instruments have further amplified the problems (Awange et al. 2016). Adding to these is the difficulty in accessing observational data, due to high costs and poor information on their availability and access conditions. These limitations justify the use of climate reanalysis products to provide continuous and distributed fields to force hydrological models. Climate reanalyses provide consistency between different atmospheric variables derived from the same numerical weather prediction (NWP) model (Ledesma and Futter 2017). Therefore, reanalysis products offer solutions for the above hydrological modeling challenges. However, they require careful evaluation when used at space scales that are not well represented by their underlying NWP models and where small amounts of observed data have been assimilated (Probst and Mauser 2022). This issue is especially critical in West Africa, specifically in Benin, the focus region for this study.

From the hydrological point of view, climatic reanalyses are good data sources. However, they often require processing to adapt them to suitable formats to suit each model's requirement, which may differ from one model to the other. For example, precipitation forcing can be event-based, hourly, daily, or monthly values. However, as spatial and temporal resolutions of physically based hydrological models have increased over the years, climate time series need to be evaluated over the cycle considered by these models. Moreover, physically based hydrological models like the parallel flow coupled hydrology–land surface model (ParFlow-CLM; Kollet and Maxwell 2005; Bodjrènou et al. 2023a) or those including land surface models (LSM), require many inputs, including precipitation, radiation, atmospheric temperature, moisture, pressure, and wind velocity at subdaily time

Corresponding author: René Bodjrenou, renebodjrenou@gmail.com

DOI: 10.1175/JAMC-D-21-0222.1

scales. From a numerical and physical point of view, these forcings, or at least certain main variables required to simulate the water balance with these models should be consistent with observations. Therefore, it is necessary to evaluate them, which is the aim of this study.

This study will focus on temperature, precipitation, and shortwave (SW) and longwave (LW) radiation. These are usually the variables used as inputs for LSMs. Rainfall is generally the main input for the hydrological budget, which impacts the variability of all other terms in the water balance (Bárdossy and Pegram 2013; Thiemig et al. 2013). SW and LW radiation are key variables in the surface energy balance and control evapotranspiration, the main output term of the hydrological budget in arid and semiarid regions (Peugeot et al. 2011). Temperature impacts the hydrological budget in many ways, especially by modifying atmospheric demand and vegetation conductance (Fan and He 2015). For such hydrological modeling usage, these variables need to be evaluated at different temporal scales (daily, seasonal, annual cycles, and decadal trends) using several evaluation metrics when compared with in situ observations for a broader understanding of the shortcomings of each reanalysis.

Several studies have evaluated reanalysis products over West Africa. Satgé et al. (2020) evaluated 23 precipitation products over three years at daily and monthly time scales. Among various reanalyses, they found that only debiased products [Water and Global Change (WATCH) Forcing Data Twentieth Century (WFD) and WATCH Forcing Data ECMWF interim reanalysis (ERA-Interim) (WFDEI); JRA adjusted atmospheric dataset (JRA-Adj)] were reliable at monthly time scales. Quagraine et al. (2020) evaluated five reanalysis products (ERA-Interim, ERA5, MERRA-2, JRA-55, and NCEP-R2) at seasonal and interannual scales. They found at a regional scale that only ERA-Interim reliably reproduced the observed wet trends but noted a high spatial variability in the values, with large differences among reanalyses. In Benin, recent evaluations of climate reanalysis products are mostly limited to a given subregion or a high temporal scale. Grenier et al. (2020) compared ERA5-Land and Climate Forecast System Reanalysis (CFSR), which has a temporal resolution of 6 h. Further studies have been carried out in the northern part of the region in the upper Oueme (Galle et al. 2018), a region of dense and well-supervised meteorological stations through the African Monsoon Multidisciplinary Analysis–Coupling of the Tropical Atmosphere and Eco-Hydrological Cycle (AMMA-CATCH) project. In their studies focusing on the upper Oueme region, Danso et al. (2019) show that the ERA5 product reliably reproduces the diurnal cycle of low-level clouds, which strongly modulates the SW evolution in the region. Dembélé et al. (2020) evaluated 102 combinations of rainfall and temperature datasets from reanalysis and satellite products over the Upper Volta basin, a basin that covers Northern Benin. Their study identified MERRA-2 as a good product for providing land water storage. However, they indicated that MERRA-2 is not always better than other products, including ERA5, at reproducing all hydrological variables. Therefore, it is challenging to deduce from these studies whether the products identified as potentially efficient in describing the climate of this northern zone of Benin are also efficient throughout the entire country. This point is especially critical because of the strong south-to-north climate gradient in the country (Fig. 1).

From the context above, this study aims to answer the following questions: 1) Does the highest spatial resolution hourly reanalysis (ERA5), capture well the temporal and spatial evolution of Benin's climate between 1981 and 2019? 2) Does it perform better than other hourly products such as WFD ERA5 (WFDE5) and MERRA-2? The answers to these questions will allow the scientific community and the various development actors in the country to rely on these reanalyses while being aware of their shortcomings. Further, this study can help to design similar reanalysis evaluations over other countries/regions in the world where data assimilation is limited and where high-quality observation datasets are insufficient.

2. Method

a. Study area

This study focuses on Benin in West Africa, which extends from the subequatorial zone to the Sudanian zone (Fig. 1). It has a warm climate with average minimum and maximum temperature ranges from 21.9° ± 3.6°C to 24.9° ± 1.8°C and from 30.5° ± 1.8°C to 34.7° ± 3.6°C, respectively, according to the southern Cotonou synoptic meteorological station and the northern Kandi synoptic meteorological station. The rainfall regime of the region is influenced by the West African monsoon (WAM), leading to three main climatic zones (Le Barbé et al. 1993). Southern Benin, located in the subequatorial zone (south of latitude ~7°N) is the wettest area, largely influenced by the Atlantic Ocean with two rainy seasons: the long rainy season from May to July and the short rainy season from mid-September to October (Amoussou et al. 2016; Bodjrènou et al. 2023a). The long rainy season receives more than 40% of the average annual rainfall (~1100 mm yr^{-1} according to rainfall data presented in this study). The Sudanian zone (north of latitude 9°N) represents the climatic regime of the north (Bodjrènou et al. 2023a). This zone has a unimodal annual rainfall cycle characterized by a dry season (November to April) with prevailing northeasterly trade winds from the Sahara (harmattan) and a wet season (June–September) with southwesterly winds from the Guinean Gulf (monsoon flow) (Gleixner et al. 2020). The region between 7° and 9°N can be considered a transition region (Sudano–Guinea zone) between the subequatorial zone and the Sudanian zone (Bodjrènou et al. 2023b). Benin has a special climate around the Atacora Mountain range (Fig. 1), which has an average altitude of 745 m average as compared with 270 m for the regional average.

b. Data description and treatment

The reanalysis products evaluated in this study (ERA5, WFDE5, and MERRA-2) have an hourly temporal resolution and cover nearly the entire period of our study (1981–2019). ERA5 is the fifth major global reanalysis produced by the European Centre for Medium-Range Weather Forecasts reanalysis (Hersbach et al. 2020). It has a 0.1° × 0.1° resolution (Muñoz-Sabater 2019). WFDE5 is a

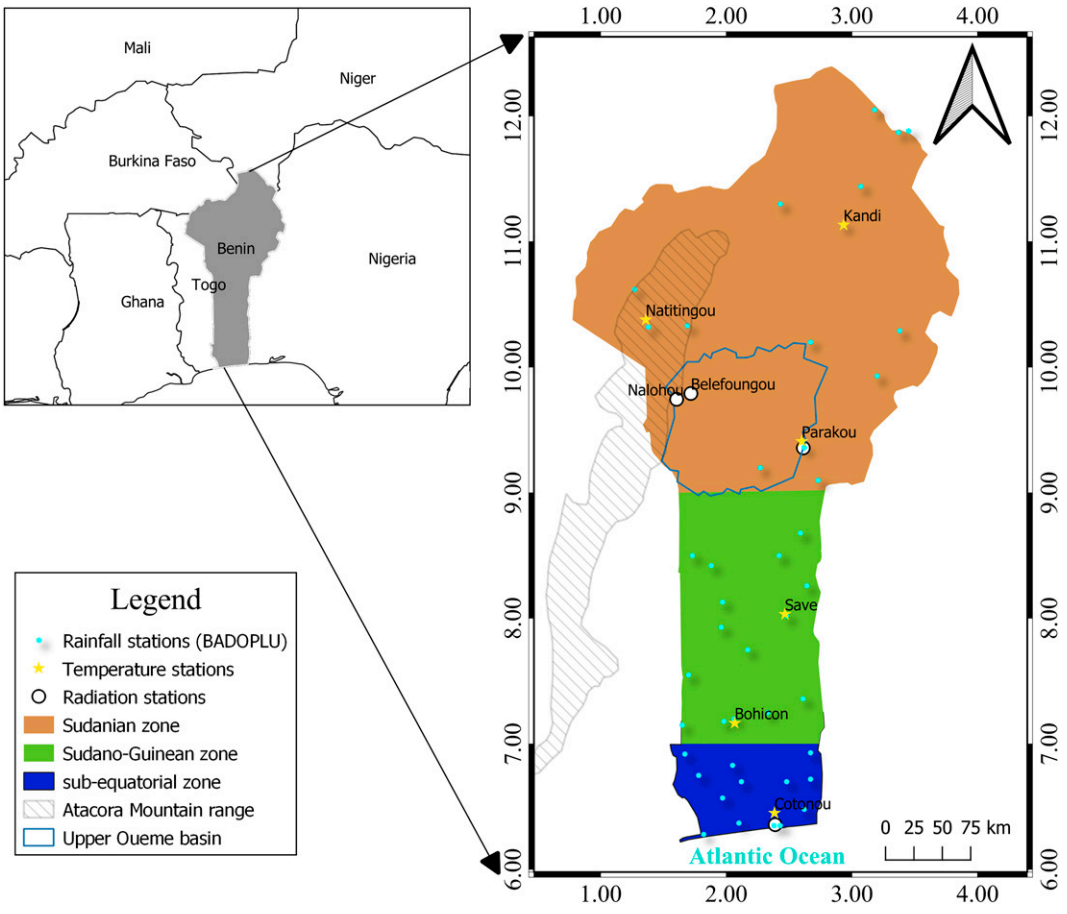

FIG. 1. Study area with different stations used (dots), the main climatic zones (colors), the Atacora Mountain range (dashed area), and the upper Oueme basin contours (blue line).

debiased version of ERA5-Land with a 0.5° × 0.5° aggregated resolution (Cucchi et al. 2020). MERRA-2 is produced by the National Aeronautics and Space Administration (NASA; Gelaro et al. 2017). It is the first reanalysis that assimilated space-based observations of aerosols and represented their interactions with other physical processes in the climate system. It is at 0.625° × 0.5° resolution (Gelaro et al. 2017). All the products were kept in their native resolution. In this study, we focus on the 2-m surface temperatures, precipitation, and incoming SW and LW radiation. These variables have the greatest impact on the water balance (Bodjrènou et al. 2023a).

To evaluate these reanalyses over the study area, several observational datasets were used (see Table A1 of the appendix for specific details of the stations). Mean, minimum, and maximum daily temperature data between 1981 and 2019 from the six synoptic stations (stars in Fig. 1) of the Meteo-Benin Agency were used. The stations are situated as follows: Cotonou station is located a coastal area within the city; Bohicon was still downtown in 2018 as well as Parakou (the old airport). Natitingou was downtown till 2012 then moved to the new airport location clearly outside the city (we kept only the data from the 1960–2012 period for consistency). Savè station is in town, but the city is not too urbanized, and Kandi station is at the airport of a very small city and still outside the city center.

Additionally, data from the national rainfall and meteorological stations (including synoptic stations) extending from 1981 to 2016 at daily time scale were also used (cyan dots on Fig. 1). These data were compiled under the name base de données pluviométriques (BADOPLU; precipitation database in West Africa) and qualified by Tapsoba et al. (2004). Data from the AMMA-CATCH observatory in the upper Oueme were also used (Galle et al. 2018). These pointwise data include hourly rainfall records from 2001 to 2019. The AMMA-CATCH database also includes SW and LW radiation recorded at 30-min intervals at two observatories: Nalohou (1.60°E, 9.74°N) and Béléfoungou (1.72°E, 9.79°N) (white dots on Fig. 1). These two stations are influenced differently by vegetation. At Béléfoungou, the station is located in a forest zone, whereas at Nalohou, the station is located in a fallow zone. Although the two stations are very close, they fall within different grid points in the reanalyses data used for the evaluation. The LW and SW radiation data from the Dynamics–Aerosol–Chemistry–Cloud Interactions in West Africa (DACCIWA) program (Fink et al. 2010; Knippertz et al. 2015) at Cotonou and Parakou were also used from the period 1999–2019. Table 1 gives more details on these observations.

TABLE 1. Description of datasets used in this study and their sources.

Variables	Sources	Periods	Resolution	Site/reference
Temperatures	Meteo-Benin	1960–2019	Daily/6 stations	http://meteobenin.bj/
Rainfall	AMMA	2001–19	30 min/29 stations	http://www.amma-catch.org/spip.php?rubrique81
	BADOPLU	1960–2016	Daily/42 stations	Tapsoba et al. (2004)
Radiations	AMMA	2005–15	30 min/2 stations	http://www.amma-catch.org/spip.php?rubrique81
	DACCIWA	1999–2019	10 min/2 stations	https://baobab.sedoo.fr/DACCIWA/

Note also that SW and LW radiation data are carefully analyzed, with many discarded, especially in the Cotonou and Parakou stations due to the lack of monitoring after the end of the DACCIWA project in 2011 and in the Béléfoungou station due to the change in height in 2015 (from 6 to 18 m). Negative values of SW and precipitation in the observed and reanalyses data are considered zero. Periods with missing data in the observations are excluded from the analysis. ERA5 is shifted 1 h backward in time, as done in WFDE5 (Cucchi et al. 2020). No further treatment is carried out in the reanalyses. For precipitation measurements, observed spatial variability is not so much pronounced on annual scale, but the monthly variability [described by Bodjrènou et al. (2023a)] leads us to the average rainfall over the subequatorial zone (latitude $< 9°$N), the Sudano–Guinean zone, and the Sudanian zone ($>9°$N).

c. *Reanalyses evaluation criteria*

The reanalyses data were evaluated at different spatial and temporal scales over the available periods (Table 1). We evaluated the products at daily, monthly, and annual time scales from 1981 to 2019. Pluri-annual trends are calculated from yearly averages, and the Mann–Kendall test is applied to check their significance at the 5% threshold. The north–south gradients were then compared to investigate the spatial variability of all variables. Spatial variability maps of the reanalyses were presented with their baseline resolution. We selected the collocated reanalysis grid point corresponding to the station location. Otherwise, the evaluation is undertaken by comparing the grid point corresponding to the station location. Spatial variability maps of WFDE5 data are presented in Fig. A1 of the appendix because this reanalysis is provided by the same group as ERA5. However, the mean values at the corresponding grid points are presented.

Several metrics, including mean absolute error (MAE) and Kling–Gupta efficiency (KGE) (Gupta et al. 2009) were used for the temporal evaluation of the products. The KGE [Eq. (1)] allows an aggregated view of the Pearson correlation (Cor), the mean μ, and the standard deviation σ ratios between reanalysis products and observations. A KGE value larger than 0.5 is considered to be a good score (Gupta et al. 2009). However, it is difficult to identify the component responsible for a given KGE value. To overcome this issue, Gupta et al. (2009) and Knoben et al. (2019) suggested decomposing the KGE submetrics and accompanying them with other evaluators. With this in mind, in addition to the stand-alone Pearson correlation calculated for all variables, we calculated the MAE, a metric that quantifies the distance between the observations and the reanalyses [Eq. (2)]. Like the KGE, the correlation is better when it is higher than 0.5; 1 is its perfect value, as opposed to 0, which is the perfect value of MAE:

$$\mathrm{KGE} = 1 - \sqrt{(\mathrm{Cor} - 1)^2 + \left(\frac{\sigma_{\mathrm{rea}}}{\sigma_{\mathrm{obs}}} - 1\right)^2 + \left(\frac{\mu_{\mathrm{rea}}}{\mu_{\mathrm{obs}}} - 1\right)^2} \quad \text{and} \tag{1}$$

$$\mathrm{MAE} = \frac{1}{n}\sum_{i=0}^{n} |Y_{\mathrm{rea}} - Y_{\mathrm{obs}}|, \tag{2}$$

where n is the sample size, Y_{rea} is the reanalysis, and Y_{obs} is the observation values.

Other complementary indicators were used for the evaluation of the reanalyses. For rainfall, we used the relative error in precipitation annual (REPA) calculated at each station [Eq. (3)]. This metric is similar to relative bias and allows us to evaluate the overestimation or underestimation of mean annual rainfall at each station (in percent). From the computation of the REPA, we can deduce the fraction of stations where the rainfall is over or underestimated, which gives integrated information on the performance of the reanalyses over the region. A REPA score in the range $]-25, +25[$ is considered to be a good rainfall estimate:

$$\mathrm{REPA} = \frac{M_{\mathrm{rea}} - M_{\mathrm{obs}}}{M_{\mathrm{obs}}}, \tag{3}$$

where M_{rea} is the average annual rainfall over the reanalyses and M_{obs} is the average annual rainfall over the observations.

These metrics have been used in numerous studies (e.g., Gleixner et al. 2020).

3. Results

a. *Temperature climatology and reanalyses comparisons*

Figure 2 shows the spatial distribution of the mean temperature in Benin for the ERA5 and MERRA-2 reanalyses. We noted an abrupt transition zone after Natitingou, north of which both reanalyses clearly show a zone with average temperatures above 28°C. Based on ERA5, which has a better resolution than both MERRA-2 and WFDE5, the Natitingou station seems to be influenced by the Atacora Mountain range (Fig. 1). This leads to a cold temperature anomaly due to the higher elevation and increased precipitation relative to the East of the country. However, the average temperature at the Natitingou station is too low in the ERA5 product when compared with the debiased one in WFDE5, which matches better with the observations.

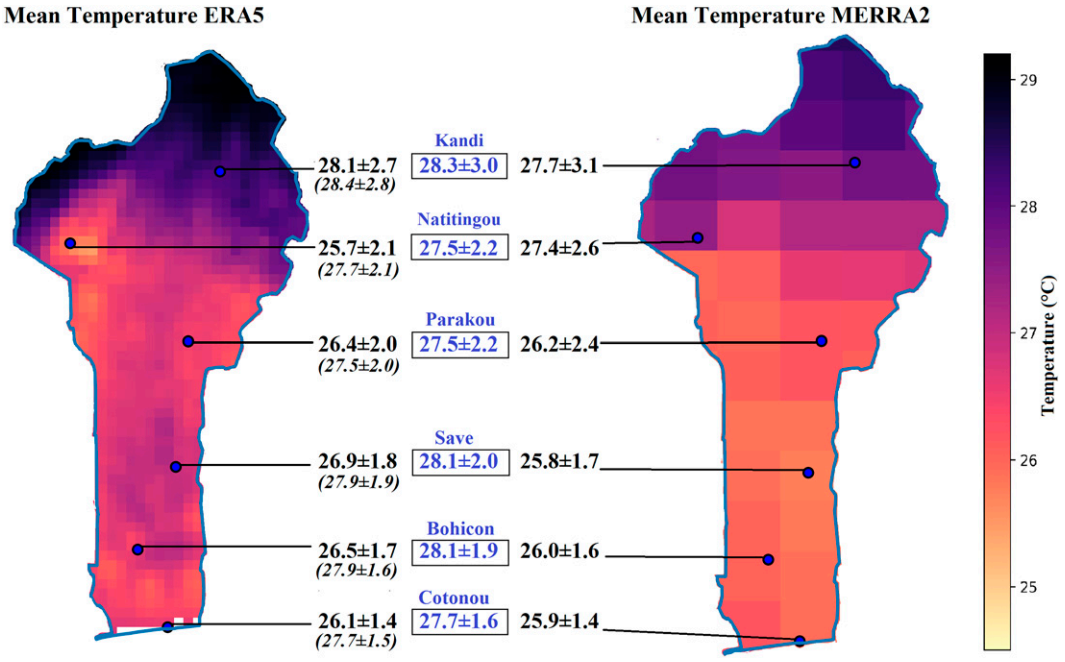

FIG. 2. Spatial distribution of mean temperature between 1981 and 2019 for (left) ERA5 and (right) MERRA-2. The boxes in the center contain the average temperature over the entire period at the six synoptic stations; ± 1 standard deviation range is also indicated. On both sides are given the average temperature of the corresponding reanalysis grid cell, ERA5 (top left), WFDE5 (bottom left in italics), and MERRA-2 (right).

Based on the observations, the temperature tends to be similar across all six weather stations (between 27.5° and 28.3°C). ERA5 and MERRA-2 reanalyses underestimate mean temperatures at all stations by an average of 1.3°C (see Fig. 5 for further details). In terms of mean temperature variability, we show an increase ranging from 1.6°C in the south (Cotonou) to 3.0°C in the north (Kandi). Both reanalyses also show increasing variations from the south station to the north station (between 1.4° and 2.7°C for ERA5 and between 1.4° and 3.1°C for MERRA-2). The WFDE5 reanalysis shows the overall best mean temperature estimate at all six stations (~0.1°C difference with observation). Its variability, however, is similar to ERA5, which underestimates it by 0.18°C on average, and better than MERRA-2, which differs by 0.25°C.

Figure 3 shows the interannual evolution of annual average temperatures at the six synoptic stations. ERA5 and MERRA-2 systematically underestimate the average temperatures at most stations, except Kandi (for both reanalyses) and Natitingou (for MERRA-2). It is clear that, although it underestimates temperature at almost all stations, ERA5's curve is more similar to the observations than the other reanalyses. For example, the observations show that the highest temperature between 1981 and 2000 occurred in 1998 at Bohicon. This high-temperature year was captured by ERA5, unlike MERRA-2 (1983) and WFDE5 (1987). Its greater consistency with observations is noted across all stations, which explains why it always presents the best correlation (Table 2).

The annual mean temperatures for the observations show a positive trend over 0.2°C decade^{-1} (Table 2). Savè and Cotonou stations have the highest increasing average temperature trends of 0.33° and 0.27°C decade^{-1}, respectively. The Savè station records the highest increasing temperature trend despite being located in a green suburban area that has not experienced any environmental change in the past decades. MERRA-2 shows a much lower trend for the five southern stations (~0.1°C decade^{-1}). ERA5 shows decade trends that are in much better agreement with observations (0.24° vs 0.21°C decade^{-1} for ERA5) when compared with those of MERRA-2 and WFDE5 (0.17°C decade^{-1}). We also note a significant trend at all observation stations. ERA5 and WFDE5 show the same result, unlike MERRA-2, which only shows a significant trend at two stations.

The minimum temperature at all stations (not shown) is underestimated by MERRA-2, except at Natitingou, and overestimated by WFDE5, except at Cotonou, located near the ocean. ERA5 underestimates the minimum temperature at Cotonou and Parakou and overestimates it at Savè and Kandi but has better correlations (0.81–0.92) than MERRA-2 (0.60–0.85) and WFDE5 (0.48–0.72). We also note that WFDE5 always overestimates maximum temperature (not shown), unlike the other two reanalyses, which underestimate it (except at Natitingou for MERRA-2). Upward trends (0.21°C decade^{-1} on observations) are captured better in ERA5 (0.22°C decade^{-1}) with the best correlations (between 0.57 and 0.86 vs 0.07–0.51 for MERRA-2 and 0.48–0.71 for WFDE5). The performance of the reanalyses on KGE and MAE metrics is reported in Fig. 5, below.

Figure 4 shows the mean annual cycle of monthly temperatures at the six synoptic stations. From the observation, the highest temperatures (minimum, mean, and maximum) occur from February

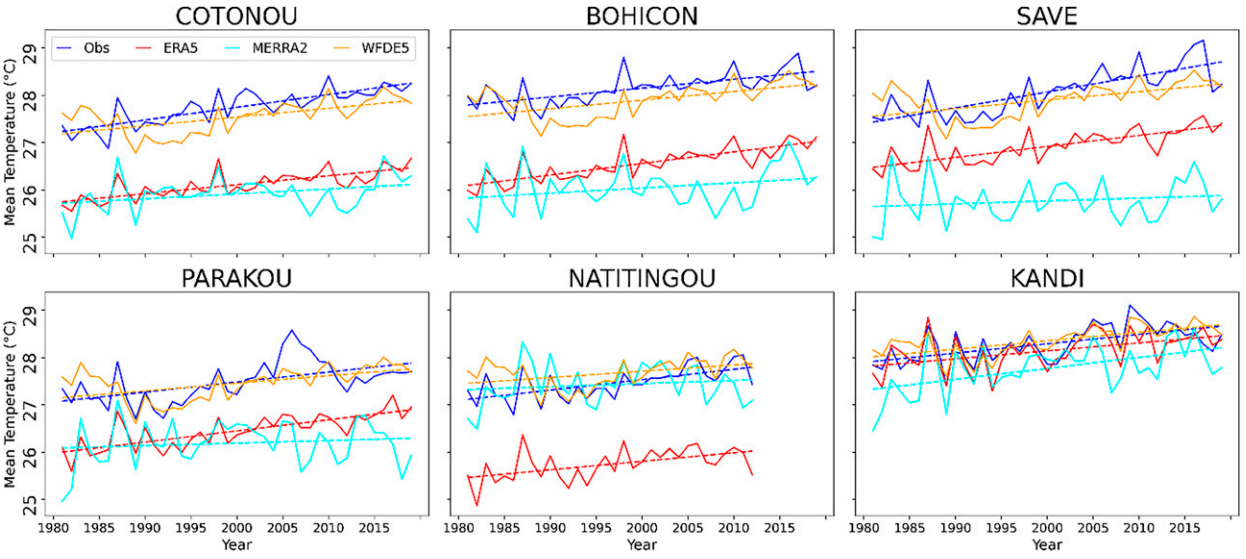

FIG. 3. Interannual mean temperature variability between 1981 and 2019 on the six synoptic stations of Benin (blue) and the corresponding grid cells in ERA5 (red), WFDE5 (orange), and MERRA-2 (cyan).

to April (FMA) and from November to December. The lowest temperatures occur in January and from July to September (JAS). August is the coldest month, with an average mean temperature of 25.7° ± 0.5°C. In contrast, March is the hottest month of the year (30.5° ± 0.8°C). All three reanalyses show these peaks of coldest and warmest months, but WFDE5 shows averages closer to observations than MERRA-2 and ERA5, which significantly underestimates the temperature (see MAE values in Fig. 5). WFDE5 and ERA5 have better correlations with the observations for the mean temperature (0.94 to 0.98 and 0.93 to 0.97, respectively). MERRA-2, on the other hand, has slightly lower correlations (0.79 to 0.96), except in Kandi, where the correlation coefficient for ERA5 is weakest. Both ERA5 and WFDE5 also show the same correlation performance (often above 0.90) for minimum and maximum temperatures, better than MERRA-2 (sometimes below 0.80). ERA5 and MERRA-2 overestimate maximum temperature, while WFDE5 underestimates it. The latter also underestimates minimum temperature at all stations, except at Cotonou, located near the Atlantic Ocean, while MERRA-2 overestimates it. Furthermore, the results show that temperature amplitudes (bar length plots) are larger in the north than in the south.

Figure 5 gives an overview of the performance of the reanalyses over Benin according to the KGE and MAE metrics at different temporal scales. This analysis helps to understand the performance of each reanalysis product in reproducing daily, monthly, and annual temperatures in the country. The best KGE scores of ERA5 and WFDE5 are obtained at the monthly scale with mean values above 0.80 (Fig. 5). The lowest KGE scores for both reanalyses are shown in the annual temperature, likely because the correlations are lowest at the annual time scale. The average MAE values of ERA5 vary between 0.54 and 1.54, which is better than MERRA-2 (1.08, 1.82). WFDE5 presents better MAE (between 0.27 and 1.15) in all cases except for the minimum temperature at the annual scale, where ERA5 has better MAE scores.

b. *Radiation climatology and reanalyses comparisons*

Figure 6 shows the spatial distribution of the mean SW and LW in Benin for ERA5 and MERRA-2. For SW, both reanalyses show a south–north gradient increasing from south to north (from darker to lighter). The observations show a similar south–north positive gradient in terms of annual average, with values ranging from 196 in Cotonou to 217 W m^{-2} in Béléfoungou. The SW values range from 201 to 236 W m^{-2} for ERA5, 179 to 222 W m^{-2}

TABLE 2. Trends (°C $decade^{-1}$) and correlations of the mean annual temperature. A significant trend at the threshold of 5% based on the Mann–Kendall test are signified with an asterisk.

	Trends (°C $decade^{-1}$)				Correlation		
Stations	Obs	ERA5	WFDE5	MERRA-2	ERA5	WFDE5	MERRA-2
Cotonou	0.27*	0.19*	0.18*	0.10*	0.86*	0.63*	0.60*
Bohicon	0.19*	0.24*	0.18*	0.11	0.87*	0.75*	0.60*
Savè	0.33*	0.23*	0.18*	0.06	0.90*	0.78*	0.51*
Parakou	0.21*	0.24*	0.16*	0.05	0.74*	0.66*	0.25
Natitingou	0.22*	0.18*	0.13*	0.07	0.85*	0.74*	0.45*
Kandi	0.20*	0.17*	0.18*	0.23*	0.82*	0.78*	0.65*

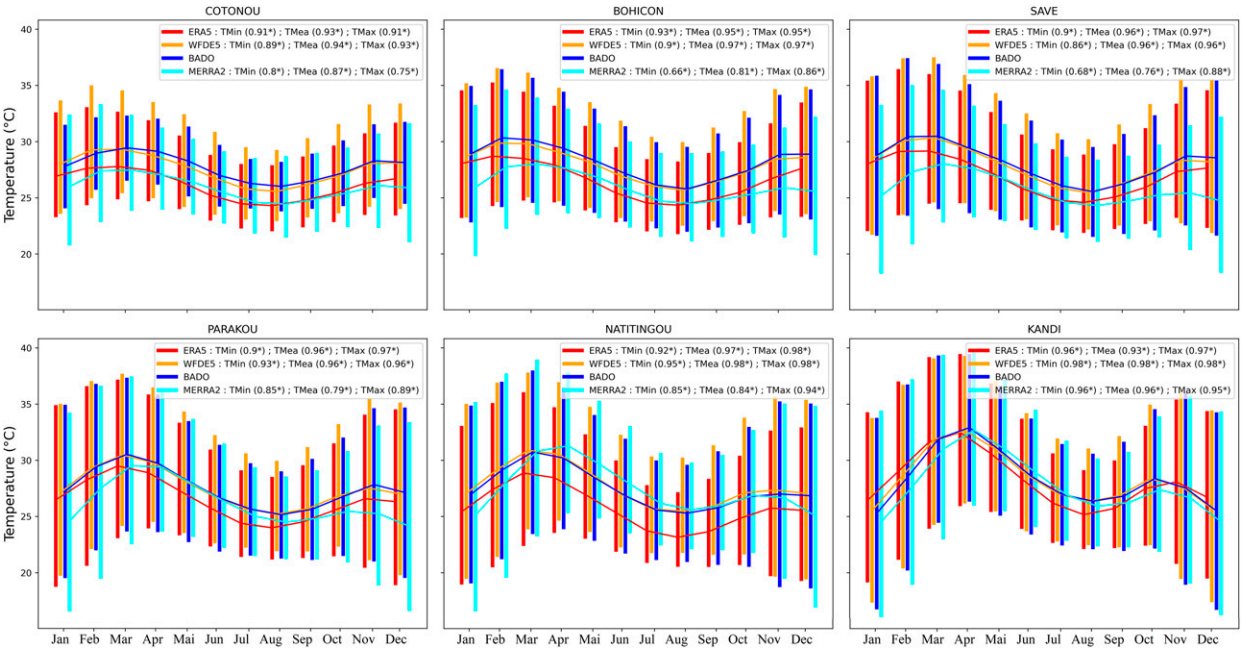

FIG. 4. Mean annual cycle of monthly temperature at the six synoptic stations. Continuous lines from January to December indicate the average monthly temperature (TMea). The upper ends of the vertical bars indicate the maximum temperature (TMax) and the lower ends are the minimum temperature (TMin). Observation is in blue, ERA5 is in red, WFDE5 is in orange, and MERRA-2 is in cyan. Correlation values are in parentheses (with an asterisk if significant).

for MERRA-2, and 195 to 230 for WFDE5 from Cotonou to Béléfoungou, respectively. The calculated MAE values at this scale are shown in Fig. 9. ERA5 shows a systematic overestimation of mean SW (~16 W m^{-2}). MERRA-2 slightly overestimates SW in the north (~6 W m^{-2}) and underestimates it in the south (~17 W m^{-2}). The standard deviations of SW are higher in the north for the three reanalyses (311 W m^{-2} for ERA5, 304 W m^{-2} for WFDE5, and 322 W m^{-2} for MERRA-2), consistent with the observations (322 W m^{-2}).

Similarly, the spatial distribution of LW in ERA5 and MERRA-2 shows a decrease from south to north, with higher values in ERA5. A slight east–west gradient can also be seen over the country in both reanalysis products. The observations show a north–south positive gradient of LW from Béléfoungou to Cotonou ranging from 403 to 421 W m^{-2}. This is captured in the reanalyses with values ranging from 392 to 418 W m^{-2} for ERA5, 382 to 405 W m^{-2} for MERRA-2, and 399 to 425 W m^{-2} for WFDE5. The reanalyses show a systematic underestimation of ~2.3 W m^{-2} for WFDE5, ~6.5 W m^{-2} for ERA5, and ~16 W m^{-2} for MERRA-2. LW variability is also better captured in WFDE5 at all stations, except at Cotonou, where the other reanalyses show values closer to observations (15 W m^{-2} vs 15 W m^{-2} for ERA5, 12 W m^{-2} for WFDE5, and 17 W m^{-2} for MERRA-2).

Figure 7 shows the mean annual cycle and interannual variability of SW and LW between 2001 and 2019 in Cotonou (south) and Parakou (north). From the observations, the SW radiation at Cotonou and Nalohou shows a typical pattern in the intertropical areas with two annual maxima and a large interannual variability (Amoussou et al. 2016). The drop in the SW radiation in the core of the rainy season is well marked at both sites from June to September. This is due to frequent occurrences of thicker clouds generated by deep convection and squall lines (Danso et al. 2019). The weaker SW radiation observed in the heart of the dry season (December and January) is likely associated with the harmattan wind, loaded with dust from the Sahara Desert, which blows over the entire country during the dry season (Danso et al. 2020b). Monthly interannual variability is generally smaller in the north than in the south except in the dry season in Cotonou, where monthly variability is small.

In the north, all reanalyses reproduce the bimodal mean SW regime with maximum values in March and November (Fig. 7, bottom left). The reanalyses substantially overestimate incoming SW, especially from December to February (DJF), by more than 25 W m^{-2} in MERRA-2 and 35 W m^{-2} in ERA5 and WFDE5. Despite this dry season effect, ERA5 reproduces the seasonal cycle and the variability well. The cycle in MERRA-2 is smoother (less annual amplitude), while WFDE5 has lower interannual variability in all months than the observations. In the south (Fig. 7, upper left), ERA5 behaves the same as in the north with a substantial bias during DJF (~40 W m^{-2}) and compares well to the observations for the rest of the year. On the contrary, MERRA-2 presents a large underestimation of SW in March and April (more than 50 W m^{-2}) and a biased seasonal cycle. WFDE5 is inferior to ERA5 in terms of interannual variability.

The seasonal cycle of LW radiation exhibits a similar bimodal annual regime that is more pronounced at Cotonou, where southern Benin has a short period with fewer clouds and no rain

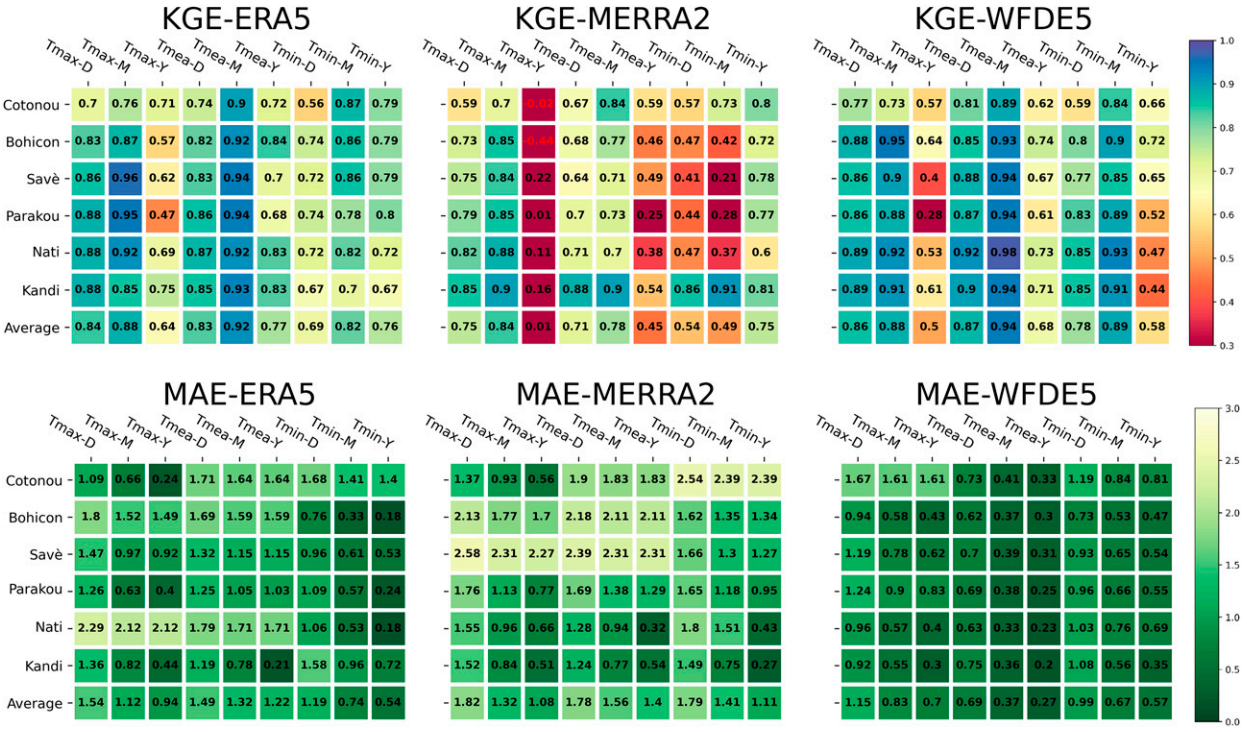

FIG. 5. (left) ERA5, (center) MERRA-2, and (right) WFDE5 reanalyses scores at daily (label D), monthly (M), and yearly (Y) time scales for Tmax, Tmea, and Tmin for (top) KGE and (bottom) MAE. Blue and green colors indicate a good performance of the reanalyses (blue for KGE and green for MAE), and red and yellow colors show a higher deviation from the observations.

in August (Fig. 7, right). The cloudy period (LW > 400 W m^{-2}) at Parakou is shorter than in the south during the last half of the year from April to October. The main differences in the LW between the two sites are seen from November to March during the harmattan period. During this period, the LW is higher over the south due to the quasi-permanent intense cloud coverage due to its proximity to the ocean. ERA5 and WFDE5 reproduce the seasonal cycle and the variability at both sites. However, WFDE5 slightly overestimates LW during the rainy season (May–November). On the contrary, MERRA-2 underestimates the incoming LW radiations all year with differences of several tens of watts per meter squared (up to 30 W m^{-2} in January).

Figure 8 details the performance of the reanalyses in terms of the diurnal cycle of radiation for January, June, and October. These months respectively correspond to the core of the dry season (harmattan winds from the north and almost no rain), the beginning of the wet (rainy) season throughout the country, and the short rainy season in southern Benin or the end of the rainy season in the north (Amoussou et al. 2016). Overall, the morning SW rise in the reanalyses is relatively well phased with the observations (zero between 1800 and 0600 local time and maximum between 1100 and 1200 local time). The reanalyses reproduce the observed SW diurnal cycle peak over the entire country in October [in Béléfoungou (815.2 W m^{-2} vs 820.8, 810.3, 759.7 W m^{-2}), Cotonou (722.0 W m^{-2} vs 687.1, 670.1, 621.2 W m^{-2}), Nalohou (796.8 W m^{-2} vs 818.1, 810.3, 742.4 W m^{-2}), and Parakou (747.6 W m^{-2} vs 793.1, 758.1, 744.5 W m^{-2}) for observed vs ERA5, NEW, WFDE5, respectively]. However, the peaks at some stations, such as Belefoungou and Nalohou for the WFDE5 and MERRA-2 reanalyses (peaks at 1100 instead of 1200 local time) and at the Cotonou station for ERA5 (peaks at 0000 instead of 1100 local time), have been shifted by one hour for this month. Finally, the reanalyses overestimate the SW at all stations in January, especially in Parakou, with a larger bias in ERA5 (174 W m^{-2} vs 165 W m^{-2} in WFDE5 and 124 W m^{-2} in MERRA-2). This is likely because it does not consider the dust transport by the harmattan. Additionally, MERRA-2 slightly overestimates SW in January but underestimates it from February to March, as has been noted in Fig. 7 (diurnal cycles not shown).

The same figure shows an underestimation of LW by all reanalyses (Fig. 8, right), as already discussed in Fig. 7. These underestimations can be as high as 50 W m^{-2} in MERRA-2 and 40 W m^{-2} in ERA5 during the midday peak, whereas WFDE5 is in better agreement with the observations. As compared with the other reanalyses and observations, MERRA-2 shows an almost flat cycle for the LW. This pronounced MERRA-2 LW daily cycle reveals clear-sky conditions in the morning and cloudy conditions from noon to midnight. This leads to a lower average LW than the observations (Fig. 7). It also must be noted that MERRA-2 data do not separate land and sea patches as done in ERA5. This can lead to large biases between observations and reanalyses over the coastal areas in our comparison. A quantified evaluation of the reanalyses' performance is presented in Fig. 9.

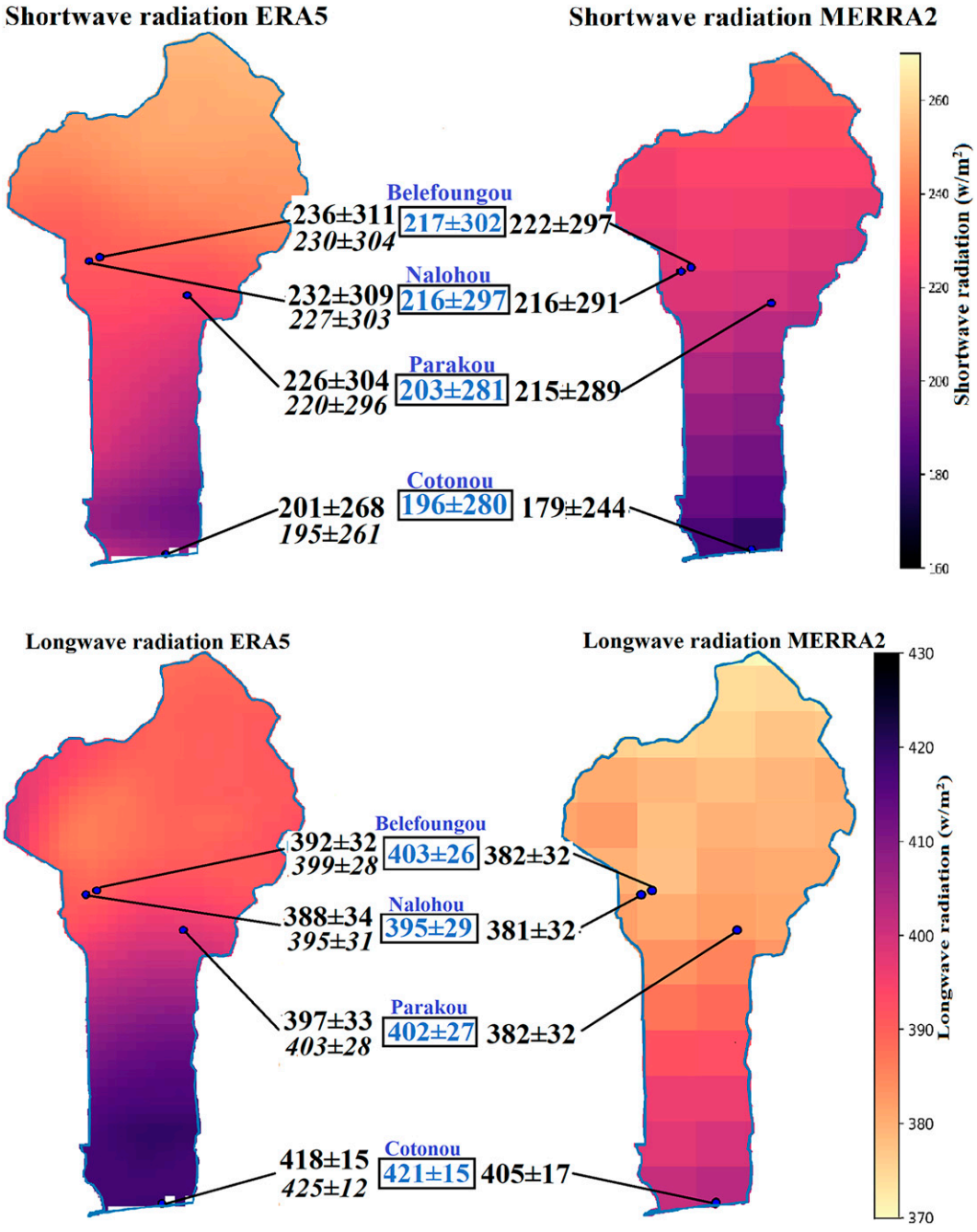

FIG. 6. Spatial distribution of the average (top) SW and (bottom) LW between 2001 and 2017 for (left) ERA5 and (right) MERRA-2. The observed values are in blue vs the reanalyses values for ERA5 (top left), WFDE5 (bottom left in italic), and MERRA-2 (right). In ascending order of numbers, the color bars go from darkest to least dark for SW (270–160) but from least dark to darkest for LW (370–430).

Table 3 shows the correlation of SW and LW radiations at daily, monthly, and annual time scales between reanalyses and observations. It confirms that, relative to MERRA-2, both ERA5 and WFDE5 have a better representation of the seasonal cycle (monthly time scale) of SW and LW radiation. At this scale, it presents correlations always higher than 0.75 for the LW and the SW except in Cotonou (SW correlation = 0.60) because of the influence of the ocean. On the other hand, the reanalyses are less effective in reproducing the radiation at the annual scale but not often significant, likely due to the small sample size.

Figure 9 shows the KGE and MAE scores at different time scales for the SW and LW. ERA5 and WFDE5 have better KGE and MAE scores than MERRA-2 (Fig. 8), indicating their potential to describe the radiation budget in this region. The better

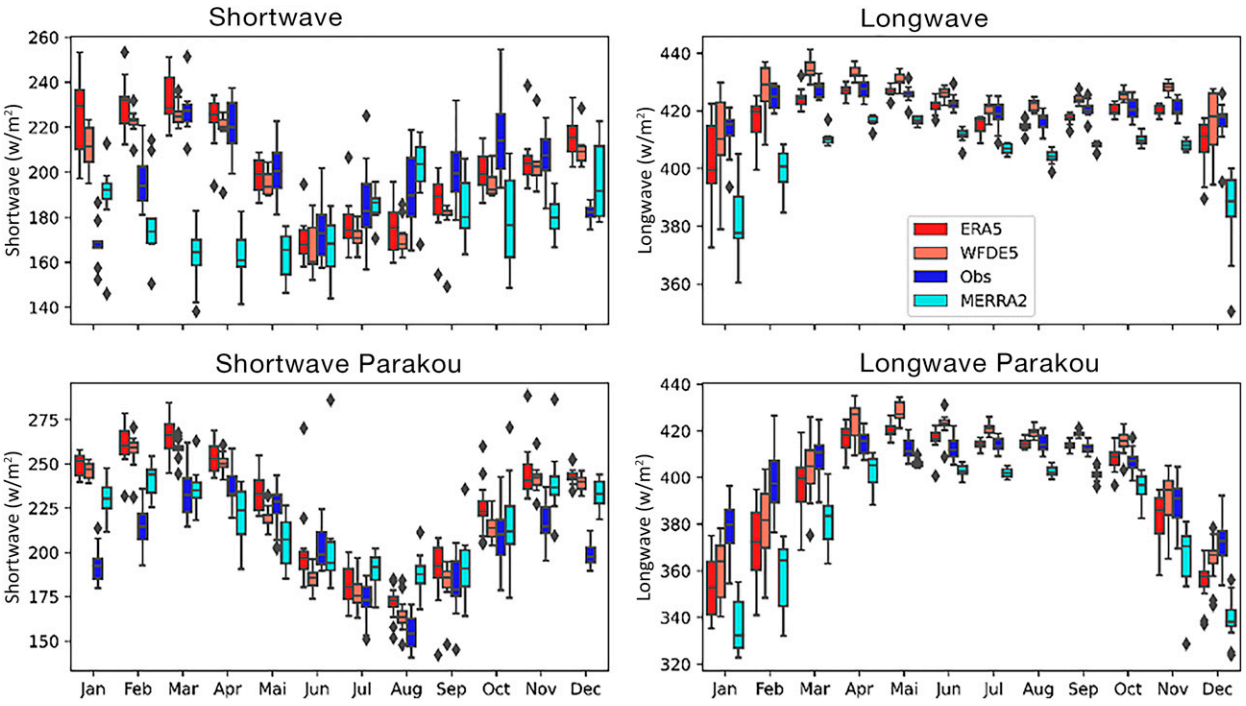

FIG. 7. Average annual cycle between 2001 and 2019 of monthly distributions (boxplots) of (left) SW and (right) LW in (top) Cotonou and (bottom) Parakou for observations (blue) and reanalyses: ERA5 (red), WFDE5 (orange), and MERRA-2 (cyan).

KGE values in ERA5 [(0.06–0.63) for SW and (0.53–0.77) for LW] and WFDE5 [(0.31–0.64) for SW and (0.50–0.72) for LW] than in MERRA-2 [(from −0.02 to 0.50) for SW and (0.37–0.53) for LW] are associated with both better correlation and MAE scores. There is no clear difference in the performance of the reanalyses from one station to another. However, the best MAE values are noted for the LW when compared with SW for the reanalysis products. This result is related to the high monthly variability of the SW radiation (Fig. 7). MAE values are better at the annual scale both for SW (average of 17 W m^{-2} for ERA5, 11 W m^{-2} for MERRA-2, and W m^{-2} for WFDE5) and LW (average of 6 W m^{-2} for ERA5, 18 W m^{-2} for MERRA-2 and 3 W m^{-2} for WFDE5) than at the monthly and daily scales.

c. *Precipitation climatology and reanalyses performances*

Figure 10 presents the spatial variability of mean annual precipitation of ERA5 and MERRA-2 over the country. We note that ERA5 and MERRA-2 present a marked north–south gradient. This is even stronger in MERRA-2, with

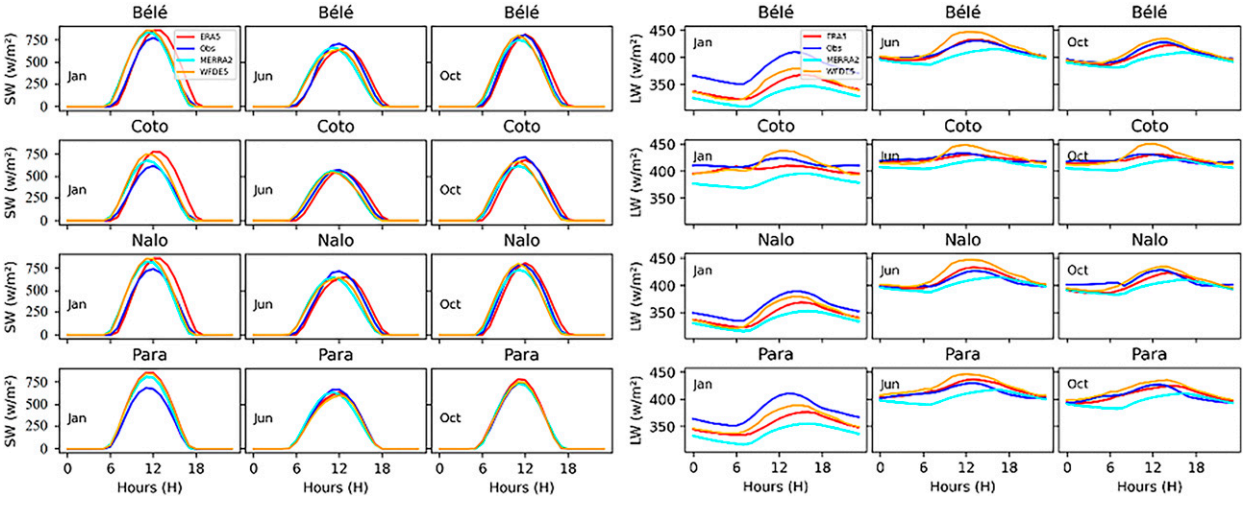

FIG. 8. Diurnal cycle of (left) SW and (right) LW at the stations of Béléfoungou, Cotonou, Nalohou, and Parakou (lines) in January, June, and October for observations (blue), ERA5 (red), WFDE5 (orange), and MERRA-2 (cyan).

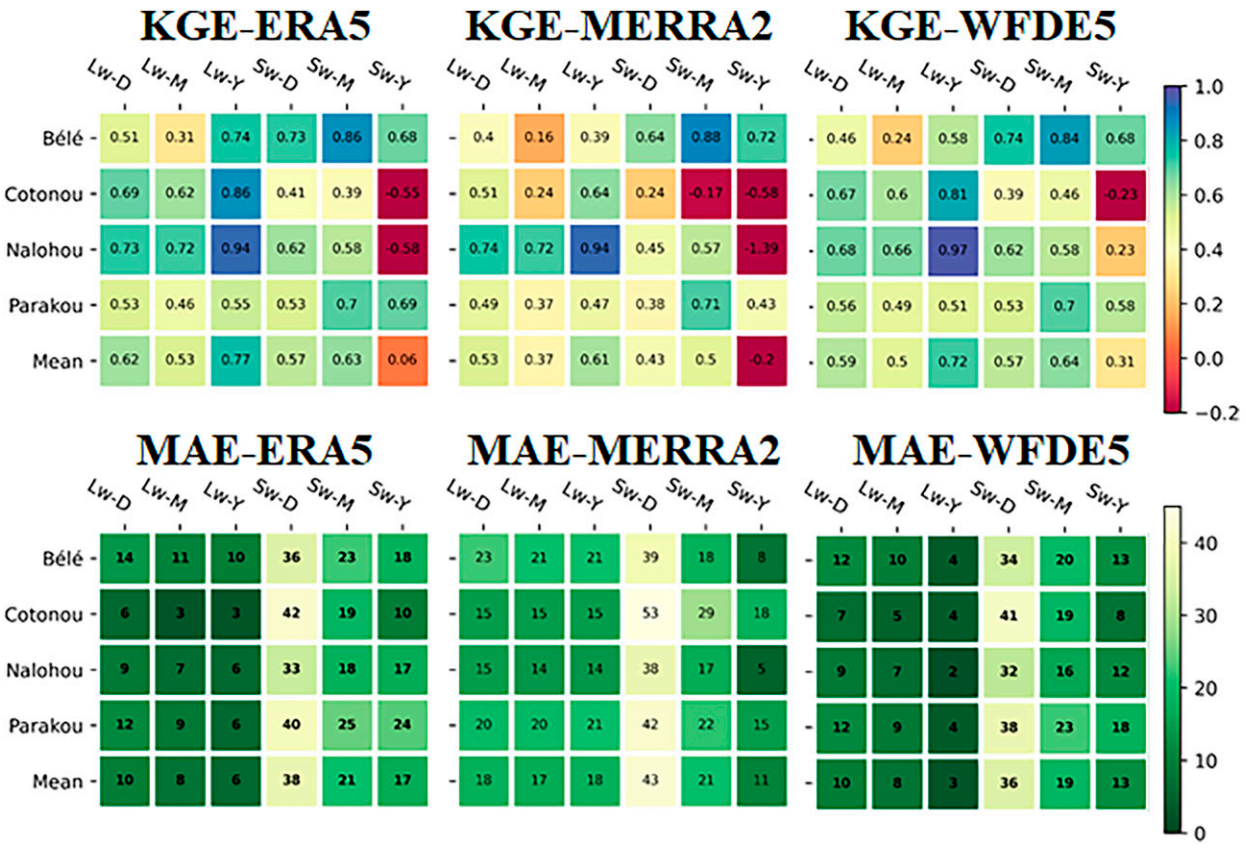

FIG. 9. (left) ERA5, (center) MERRA-2, and (right) WFDE5 reanalysis scores for LW and SW radiation for (top) KGE and (bottom) MAE for ERA5 and MERRA-2 at daily (D), monthly (M), and yearly (Y) time scales. Blue (for KGE) and green (MAE) colors indicate a good performance of the reanalyses, and red and yellow colors show a higher deviation from the observations.

precipitation up to 1600 mm yr^{-1} in the south and less than 600 mm yr^{-1} in the north. ERA5 shows an east–west gradient in central Benin that is slightly present in the observations (i.e., a higher value in Natitingou than in Parakou). From the observation, precipitation values range from 900 (north) to 1300 (south) mm yr^{-1}. Thus, we can say that the coastal region is the wettest area, while the north is the driest, with annual precipitation amounts decreasing rapidly north of 11°N. In this region, all reanalyses underestimate the average annual precipitation (~200 mm for ERA5, ~50 mm for WFDE5, and ~500 mm for MERRA-2). In the southern part of the country, MERRA-2 presents a poor estimation of the annual precipitation when compared with other reanalyses (1600 mm yr^{-1} vs 1300 mm yr^{-1} in observation, ERA5, and WFDE5). We also note that the east–west gradient (difference in mean between the Natitingou and Parakou stations) in ERA5 (70 mm) is similar to the observation (42 mm) as compared with WFDE5, which has an extremely strong gradient (154 mm) and MERRA-2 with no

TABLE 3. Correlations on SW and LW between 2001 and 2019 at different time scales. A significant correlation at the threshold of 5% is indicated by an asterisk.

	Béléfoungou			Cotonou			Nalohou			Parakou		
Scale	ERA5	WFDE5	MERRA-2	ERA5	WFDE5	MERRA-2	ERA5	WFDE5	MERRA-2	ERA5	WFDE5	MERRA-2
						Longwave radiation						
Annual	0.83	0.77	0.83	−0.15	−0.16	−0.3	0.98*	0.98*	0.98*	0.55*	0.52*	0.52*
Monthly	0.93*	0.91*	0.93*	0.76*	0.78*	0.64*	0.97*	0.96*	0.97*	0.9*	0.89*	0.89*
Daily	0.79*	0.78*	0.79*	0.73*	0.73*	0.65*	0.93*	0.93*	0.93*	0.83*	0.82*	0.81*
						Shortwave radiation						
Annual	0.56	0.55	0.68*	0.98*	0.98*	0.98*	0.4	0.42	0.44	0.73*	0.63*	0.47
Monthly	0.89*	0.89*	0.86*	0.6*	0.65*	0.31*	0.81*	0.79*	0.56*	0.83*	0.78*	0.72*
Daily	0.75*	0.75*	0.65*	0.47*	0.47*	0.27*	0.63*	0.63*	0.46*	0.56*	0.54*	0.39*

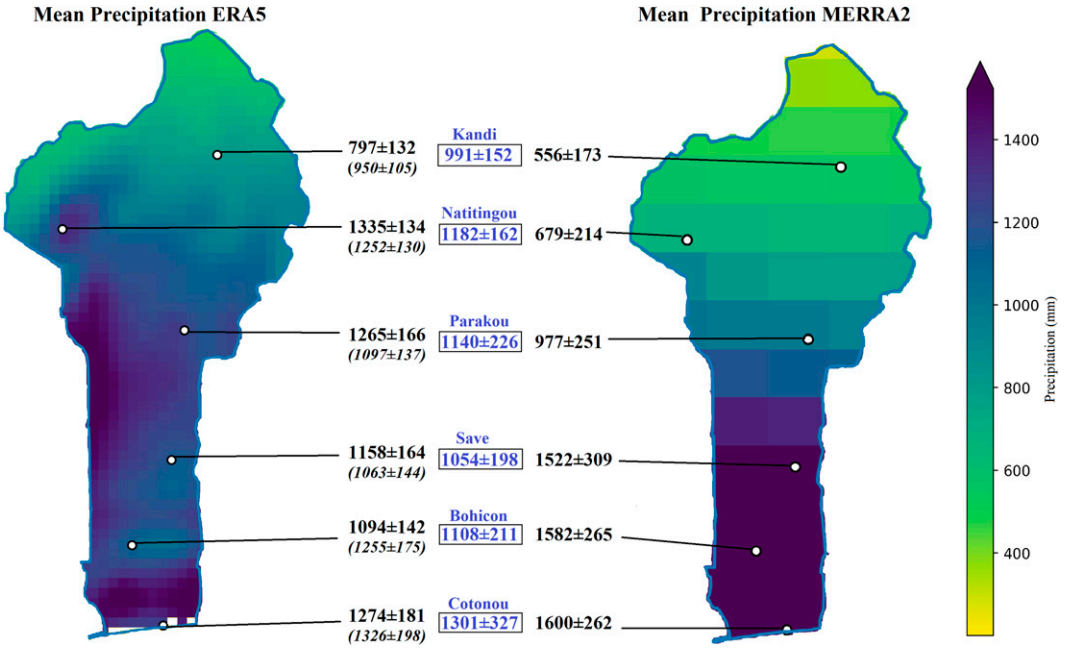

FIG. 10. Spatial variability of mean annual precipitation in Benin for (left) ERA5 and (right) MERRA-2.

gradient. This may be due to the lower resolution of MERRA-2 and WFDE5 than of ERA5. Apart from the Cotonou station, where ERA5 and WFDE5 show interannual variability over 120 mm, likely due to the influence of the ocean, the reanalyses bias is ~52 mm for MERRA-2 and WFDE5 versus ~42 mm for ERA5.

Figure 11 shows the mean annual cycle and interannual variability of precipitation for the three climate zones in Benin (Fig. 1). The mean annual precipitation in the subequatorial zone is overestimated by more than 100 mm in all reanalyses (1115 mm for observations vs 1224 mm for WFDE5, 1337 for ERA5, and 1578 for MERRA-2). This overestimation is present in all years except for a few years in ERA5 (2009 to 2013) and WFDE5 (1990, 2016, and 2013). WFDE5 shows the best performance in terms of correlation (0.91*; the asterisk indicates significance) and nonsignificant positive trend (4.24 mm yr^{-1}, in line with observation 4.84 mm yr^{-1}) when compared with ERA5 (correlation = 0.49* and trend = −5.93*) and MERRA-2 (correlation = 0.56* and trend = 13.37*). Performance is almost identical in the Sudano–Guinean zone. However, in the Sudanian zone, improvements were observed for ERA5, whose average is closest to the observations (1002 mm vs 981 mm for ERA5, 1076 mm for WFDE5, and 679 mm for MERRA-2). Similar improvements were noticed for the trend in MERRA-2 (Table 4). Note that none of these trends are significant (at the 5% level), which is not surprising given the low signal-to-noise ratio of annual precipitation in this region.

The annual cycles for both observations and reanalyses (Fig. 11, right) clearly show the bimodal precipitation regime in the subequatorial zone and the unimodal cycle in the north (Sudanian zone). All reanalyses perform well during the dry season (November–February), during which both the observations and reanalyses show a virtual absence of precipitation, particularly in the Sudanian and Sudano–Guinean zone. The rainfall peak in northern Benin is well captured in all reanalyses (average in August equal to 244 mm for ERA5, 239 mm for WFDE5, 225 mm for observations, and 190 mm for MERRA-2), while the two rainy season peaks in southern Benin (June and October) are improperly captured. MERRA-2 shows a first peak in July (228 mm) instead of June (ERA5 = 188 mm, WFDE5 = 198 mm, BADO = 200 mm, and MERRA-2 = 185). The second peak in the reanalyses is shown in September (ERA5 = 147 mm, WFDE5 = 157 mm, observation = 123 mm, and MERRA-2 = 250 mm), while the observation peak is in October (136 mm). Generally, WFDE5 better reproduces the seasonal cycle and the interannual variability at the monthly time scale [correlation equal to ~0.96* vs (0.83 to 0.95) for ERA5 and (0.62, 0.86*) for MERRA-2].

Figure 12 shows the performance of the three reanalyses against the AMMA-CATCH data of the upper Oueme basin (Fig. 1). The observed mean annual precipitation is 1195 mm for longitude = [1.5°, 2.0°] versus 1181 mm for longitude = [2.0°, 2.5°], demonstrating a slight east–west gradient (Fig. 10). This gradient is also visible in ERA5 (from 1313 to 1167 mm) and WFDE5 (from 1244 to 1186 mm) but absent in MERRA-2 (from 815 to 777 mm). Contrary to MERRA-2, ERA5 and WFDE5 show an opposite trend and lower correlation on interannual precipitation (Table 4), but they present a good correlation on the monthly scale (above 0.90, contrary to MERRA-2, which is always less than 0.80). Both reanalyses also present a better annual cycle with a peak in August and lower difference at longitude = [2.0°, 2.5°] (1 mm for ERA5, 29 mm for WFDE5, and 40 mm for MERRA-2).

The cumulative frequency (Fig. 12, right) indicates that rainfall higher than 5 mm h^{-1} represents more than 0.7% of

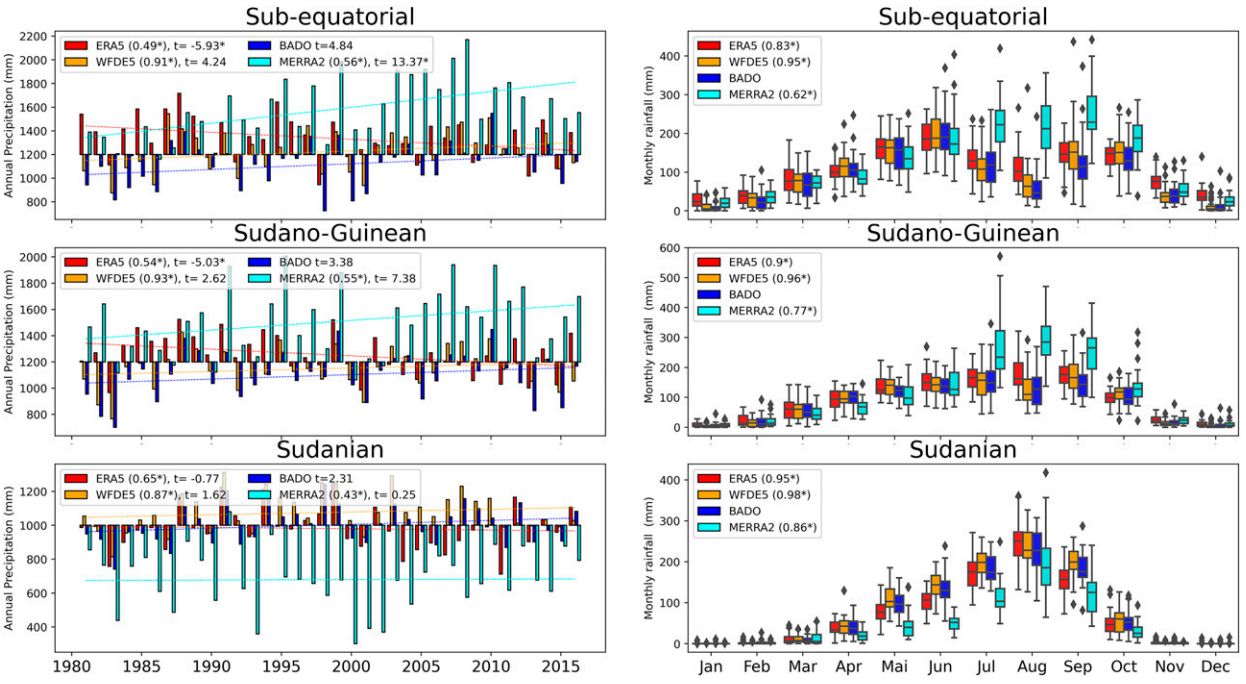

FIG. 11. Interannual precipitations (with the trend) and the mean annual cycle variability of the mean annual precipitation on BADOPLU (blue), ERA5 (red), WFE5 (orange), and MERRA-2 (cyan) between 1981 and 2016. The boxplots represent the interannual variability on the mean precipitation. Here, t = trend, and the values in parentheses are for correlation, with an asterisk if significant.

the sample of rainfall in the observations. However, they represent less than 0.3% in the reanalyses (~0.29% for ERA5 and WFDE5 and ~0.16% for MERRA-2). The percentage of rainfall higher than 0 mm h^{-1} in the reanalyses is much higher than in the observations (~8% vs ~18% for ERA5, ~14% for WFDE5, and ~27% for MERRA-2). This suggests that the reanalyses tend to simulate frequent low-intensity events. The reanalyses reach the 99% frequency threshold at rainfall intensities of 13 mm h^{-1} for ERA5 and WFDE5 and 26 mm h^{-1} for MERRA-2, while the observation data are at less than 90% of cumulative frequency for rainfall intensities below 30 mm h^{-1}. The observed very high rainfall intensities are not captured in the reanalyses.

Table 4 presents the percentage of stations for which some evaluation indicators were looked at. This uses the observed data to determine the better reanalysis products in their representation of the precipitation at the stations. From this table, correlation coefficients higher than 0.5 are found in more than 80% of the stations for WFDE5 and ERA5, against less than 80% for MERRA-2. Similarly, the best estimate of the mean annual rainfall (REPA $\in]-25, 25[$) is observed in more than 90% of the stations for WFDE5, more than 70% of the stations for ERA5 as compared with MERRA-2, which reproduces rainfall values in less than 25% of the stations. We also show that the performance of all reanalysis products is better, especially for the REPA metric, in the Sudano–Guinean zone (93.3% for ERA5, 100% for WFDE5, and 26.7% for MERRA-2) than in the subequatorial zone (30.8% for ERA5, 100% for WFDE5, and 15.4% for MERRA-2) or

TABLE 4. Evaluation of mean annual precipitation at different climate zones by correlation, KGE, trends, and REPA metrics.

	Subequatorial (13)			Sudano-Guinean (15)			Sudanian (15)			Upper Oueme (42)		
Indicators	ERA5	WFDE5	MERRA-2	ERA5	WFDE5	MERRA-2	ERA5	WFDE5	MERRA-2	ERA5	WFDE521q	MERRA-2
Cor ≥ 0.50	84.6	100	92.3	93.3	100	86.7	73.3	93.3	40.0	9.5	4.8	2.4
Cor < 0.50	15.4	0.0	7.7	6.7	0.0	13.3	26.7	6.7	60.0	90.5	95.2	97.6
KGE < 0.5	15.4	0.0	0.0	0.0	0.0	6.7	20.0	0.0	40.0	100	100	100
KGE ≥ 0.5	84.6	100	100	100	100	93.3	80.0	100	60.0	0.0	0.0	0.0
REPA ≤ -25	7.7	0.0	0.0	0.0	0.0	0.0	6.7	0.0	80.0	100	100	100
REPA $\in]-25, 25[$	30.8	100	15.4	93.3	100	26.7	93.3	80.0	20.0	0.0	0.0	0.0
REPA $> 25\%$	61.5	0.0	84.6	6.7	0.0	73.3	0.0	20.0	0.0	0.0	0.0	0.0
Same trend	38.5	76.9	61.5	66.7	93.3	73.3	60.0	80.0	93.3	64.3	61.9	76.2
Opposite trend	61.5	23.1	38.5	33.3	6.7	26.7	40.0	20.0	6.7	35.7	38.1	23.8

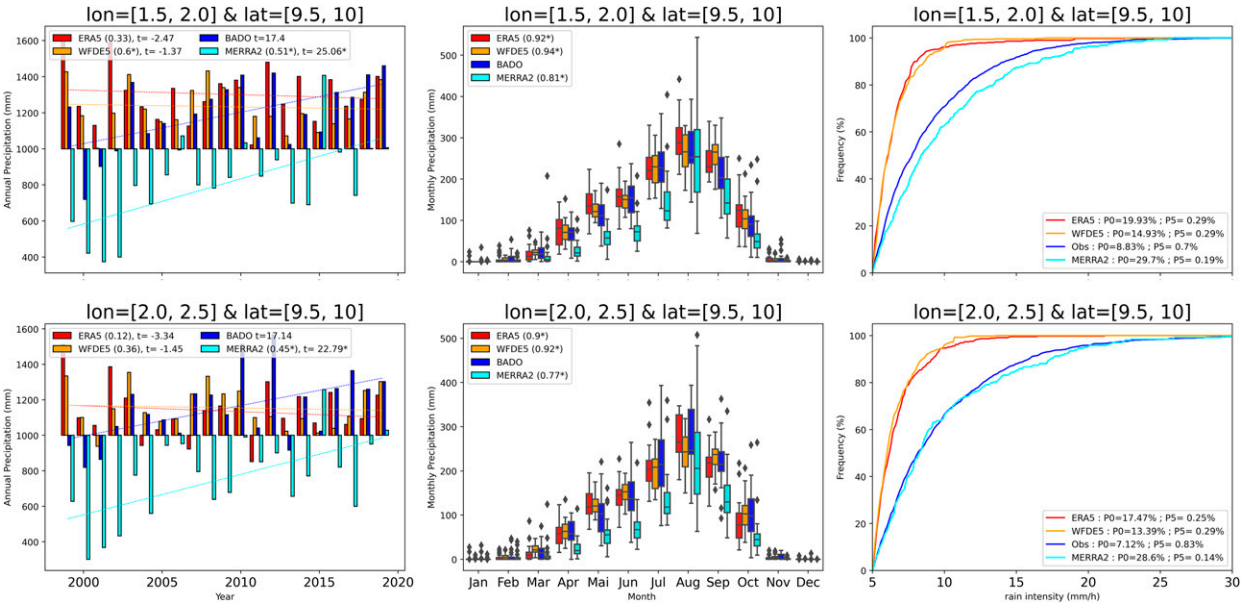

FIG. 12. Performance of ERA5 (red), WFDE5 (orange), and MERRA-2 (cyan) reanalyses based on AMMA-CATCH data (blue) for the upper Oueme between 2001 and 2019, for (left) the annual precipitation, (center) the monthly precipitation, and (right) the cumulative frequency of rainfall intensities greater than 5 mm h^{-1}. Numbers in parentheses indicate the correlation between observation and reanalyses; t is trend, P0 is precipitation percentage greater the 0 mm h^{-1}, and P5 is precipitation percentage greater the 5 mm h^{-1}.

the Sudanian zone (93.3% for ERA5, 80% for WFDE5, and 20.0% for MERRA-2).

In upper Oueme, all of the reanalysis products perform poorly in all metrics. REPA $\in]-25, 25[$ is equal to 0%, correlations superior to 0.5 is lower than 10%, and KGEs superior to 0.5 is equal to 0%. This result is likely linked to the fact that an average of 10 observation stations are compared at the same reanalysis point. In addition, these results are not statistically significant (Fig. 12, left).

4. Discussion

Our discussion is divided into four points. The first point is devoted to the comparison technique, followed by a discussion on temperature, radiation, and precipitation in the second, third, and fourth points, respectively. We noted that horizontal resolution is a factor that significantly influences the performance of the reanalysis products. Grid points in reanalysis products cover large areas. Thus, comparing point observations with those grid points may not necessarily be representative (Amoussou et al. 2016; Nkrumah et al. 2019). The horizontal resolutions generally determine the distance between the point selected in the reanalysis and the station point. This may be the reason why MERRA-2 (resolution 0.5° × 0.625°) always has poorer performance than ERA5 (resolution 0.1° × 0.1°). For example, when compared with the Bohicon station, the center of the grid points from the station coordinate in ERA5 is 5.2 km, WFDE5 is 22.4 km, and MERRA-2 is 28.2 km. This technique sometimes leads to comparing a single reanalysis grid point with several different observation points and vice versa. Such is the case of the AMMA-CATCH dataset (grid longitude = [1.5°, 2.5°] and latitude = [90°, 10°]), with which we compare 42 observation stations with four reanalysis points in WFDE5 and MERRA-2. This means that one grid point in MERRA-2 or WFDE5 may have been used for comparison with several observation stations. This situation is less likely with ERA5 owing to its higher resolution and higher number of grid points (100 points). We did not account for observation uncertainties that can be significant (Gupta and Maravelias 2019). Analysis of the coherences between the observed variables (temperature, radiation, and precipitation) may appear necessary in this area where the data are highly criticized (Clark et al. 2009). However, this was not accounted for. More specifically, for the Cotonou station, we commented several times on the effect of the station's proximity to the ocean and the associated discrepancies between the observations and reanalyses. However, our conclusions about the intense cloudiness in the coastal areas and their impacts on radiation are well shared by the community (e.g., Danso et al. 2019). We also commented on the results in the mountainous region, especially in Natitingou, where specific discrepancies could be associated with the location of the observation station. In general, synoptic stations in Benin are located in urban and suburban areas. Thus, they can record point temperatures higher than the average in the reanalyses because of the urban heat island related to urbanization, infrastructure construction, etc. (Lin and Xu 2018).

Second, we show that the reanalyses follow the observed south–north temperature gradient, which is consistent with studies by Badameli and Dubreuil (2015) and Oguntunde et al. (2012), conducted in neighboring countries located to the west (Togo) and east (Nigeria) of Benin. According to these studies,

the north is the hottest zone, with average temperatures about 3°C warmer than the South. The temperature showed an upward trend in the same range as the 0.2°C decade^{-1} global warming (Vose et al. 2005) and observed in the West African subregion (Atedhor et al. 2011, Nigeria; Loua et al. 2019, Guinea; De Longueville et al. 2016, Burkina-Faso). There are some discrepancies at the annual, monthly, and daily scales that may be associated with reanalyses biases and uncertainties in the measurements. The WFDE5 temperature (minimal, maximal, and mean) is very well in agreement with observations at different time scales, likely due to the efficiency of corrections applied (Cucchi et al. 2020). The poorer correlations than those of ERA5, which are sometimes identified in WFDE5, may be explained by the fact that the corrections are applied to ERA5-Land, which has a resolution of 0.25° × 0.25°, and not to the ERA5 used in this study (Hersbach et al. 2020).

In our study, the spatial variabilities of radiation are consistent with Patchali et al. (2020), who observed higher radiation in the north than in the south of Togo. It is also consistent with the studies of Danso et al. (2020b), who showed that attenuation of incoming solar radiation is maximum in August. The reanalyses showed strong LW over the south relative to the north. Simultaneously, the SW is higher in the south outside the dry season. This result agrees with the findings of Babić et al. (2019), who showed that West Africa is characterized by a high frequency of low-level nocturnal stratus clouds in the atmospheric boundary layer during the monsoon season. Indeed, the rainy season is favorable for low-level stratus formation, a phenomenon that considerably reduces the SW in West Africa (Danso et al. 2020a). This can explain the systematic negative bias in the reanalyses SW considering the inability of the models used to build the reanalyses to accurately reproduce clouds due to low resolutions and poor representation of the microphysical processes (Ebert et al. 2007; Maidment et al. 2013). In the south, Neher et al. (2020) suggested that the radiation in southern West Africa could be influenced by the more dominant urbanization at low altitudes in this region, which could increase aerosols emission and, thus, the formation of clouds through condensation nuclei. The reanalyses are not able to accurately reproduce the observed cloud cover, which impacts the radiation budget. Dust effect could also play a role in the negative biases found in the reanalyses in the northern part of the country (Parakou, Béléfoungou, Nalohou) during the dry season.

Precipitation results are highly debatable, especially on the annual time scale. There is a positive north–south gradient and a slight positive west–east gradient, which are both visible in the analyses (markedly in ERA5 and WFDE5) and observations (BADOPLU and AMMA-CATCH). Similar results were found by Amoussou et al. (2016), who assessed the spatial variability of rainfall in Benin for all months. On the interannual evolution of precipitation, we show the rainfall trends in Benin are increasing (slightly between 1981 and 2016 and strongly between 1999 and 2019) in a nonsignificant way. Although this is not the topic of this study, we showed that WFDE5 can represent both the trend and the interannual variability, which may be due to the effectiveness of the correction applied (Cucchi et al. 2020). The bimodality of rainfall in southern Benin is in line with the study of Lawin et al. (2019). According to the authors, the two rainy season peaks merge as latitude increases. The low rate of rainfall above 5 mm h^{-1} in the observations as compared with reanalysis is explained in the study of N'Tcha M'Po (2016) by the nonsensitivity of the rain gauges. The quantity of observed events over 5 mm shows that even after the bias correction, WFDE5 is still not effective in accurately reproducing intensity. This may be because the bias correction applied in this reanalysis consists of suppressing smaller rainfall events until the monthly rain amount corresponds to the observation (Cucchi et al. 2020; Bodjrènou et al. 2023a).

5. Conclusions and recommendations

In this study, we evaluate the ability of the ERA5, WFDE5, and MERRA-2 to reproduce the characteristics of temperature, incoming SW and LW, and precipitation over Benin from 1981 to 2019 using ground-based measurements as references. Spatial variabilities, interannual trends, and mean annual cycle of temperature are reproduced well by the different products. We further analyzed the daily time series, which exhibits some differences associated with identified issues with climate modeling (cloud cover and associated precipitations).

SW latitudinal gradient of reanalyses is consistent with the average values observed, and the latter is very similar to the averages in the reanalyses at all stations and time scales, except the coastal region where all products suffer from a deficit of incoming solar radiation. We also noted an excess of LW, which is likely associated with too much cloud cover at every time scale.

North of 11°N, Benin has a fairly spatially homogeneous precipitation distribution that constitutes an anomaly in the regional south–north gradient. This is due to the Atacora Mountain range located west of Benin, which is not represented well in WFDE5 and MERRA-2 owing to their coarse resolution. The precipitation homogeneity is then poorly reproduced in ERA5 and MERRA-2, which still present regional precipitation gradient over Benin. However, ERA5 can represent the bimodal rainfall regime south of 9°N and the unimodal rainfall regime north of 9°N, which is not the case for MERRA-2. WFDE5 is the best product in terms of spatial distribution and is consistent with the annual and monthly averages of observations. It is also shown that all three reanalysis products present a low hourly rainfall distribution.

We found that no product is simultaneously better in both spatial and temporal representation at all time scales. Consequently, there is not one best product for the simulation of water balance. Each product has its shortcomings that may be absent in others. However, we recommend using ERA5 or WFDE5 depending on the resolution of the hydrological model to be deployed or the objective pursued.

On the other hand, using WFDE5 precipitation still requires CDF matching if one hydrological model is sensitive to rain intensity because it has a low hourly rainfall distribution like the other reanalyses. Other methods deemed useful can also be used. However, it would be ideal to retain the annual and monthly totals when considering using this reanalysis for

hydrological modeling in Benin. We did not run hydrological models to evaluate their ability to reproduce hydrological outputs, including stream flows, soil moisture, water table recharge, or evapotranspiration. This will be done in future studies. This study contributes to the ongoing discussion on using climate reanalysis products for various time-scale hydrological modeling. We advise such an approach for data-scarce regions.

It is also important to note that this study does not provide any information on the performance of reanalyses in reproducing the diurnal temperature cycle. Therefore, we recommend that this be considered in future studies to ensure that the reanalysis temperatures are suitable for simulating water balance terms at high temporal (hourly) scales.

Acknowledgments. The authors thank the technical and financial partners involved in this study. These are mainly the OmiDelta Project of the National Water Institute (INE-Benin), the Institute of Research for Development (IRD-France), Embassy of France, and the Institute of Environmental Geosciences of the University of Grenoble Alpes (IGE-UGA).

Data availability statement. All data used during this study are openly available from various sources, as shown in the reference column of Table 1.

APPENDIX

Additional Table and Figure

Table A1 presents a list of the stations used in this study along with some of their associated characteristics. Figure A1 shows spatial variability maps of WFDE5 data.

TABLE A1. List of stations. "name" is the station name, lat and lon indicate latitude (°N) and longitude (°E), Meteo" is the Meteorological Agency of Benin, "year" corresponds to the year in which the station was installed, and "source" corresponds to the provenance of the data.

No.	Name	Lat	Lon	Year	Source	No.	Name	Lat	Lon	Year	Source
		Temperature						*Precipitation*			
1	Bohicon	7.17	2.07	1940	Meteo	17	Gaya	11.88	0.45	1931	Badoplu
2	Cotonou	6.35	2.38	1940	Meteo	18	Gouka	8.13	1.97	1969	Badoplu
3	Kandi	11.13	2.93	1940	Meteo	19	Popo	6.28	1.82	1921	Badoplu
4	Natitingou	10.38	1.36	1940	Meteo	20	Kalale	10.29	3.38	1957	Badoplu
5	Parakou	9.35	2.60	1940	Meteo	21	Kandi	11.13	2.93	1921	Badoplu
6	Savè	10.32	1.38	1940	Meteo	22	Karimama	12.05	3.18	1976	Badoplu
		Radiation				23	Ketou	7.36	2.61	1951	Badoplu
1	Béléfoungou	9.79	1.72	2001	DACCIWA	24	Kokoro	8.26	2.64	1969	Badoplu
2	Cotonou	6.36	2.39	2001	DACCIWA	25	Kouande	10.33	1.69	1932	Badoplu
3	Nalohou	9.74	1.60	2001	AMMA	26	Lonkly	7.15	1.65	1956	Badoplu
4	Parakou	9.36	2.61	2001	AMMA	27	Malanville	1.87	3.37	1942	Badoplu
		Precipitation				28	Natitingou	0.32	1.38	1921	Badoplu
1	Oueme	Upper basin		1999	AMMA	29	Niaouli	6.7	2.12	1941	Badoplu
2	Abomey	7.18	1.98	1921	Badoplu	30	Nikki	9.93	3.2	1921	Badoplu
3	Adjohoun	6.7	2.48	1921	Badoplu	31	Okpara	9.1	2.73	1957	Badoplu
4	Agouna	7.55	1.7	1969	Badoplu	32	Ouesse	8.5	2.42	1964	Badoplu
5	Alfakoara	11.44	3.07	1969	Badoplu	33	Ouidah	6.37	2.1	1921	Badoplu
6	Aplahoue	6.92	1.67	1922	Badoplu	34	Parakou	9.36	2.62	1921	Badoplu
7	Banikoara	11.3	2.43	1954	Badoplu	35	Pira	8.5	1.73	1969	Badoplu
8	Bante	8.42	1.88	1942	Badoplu	36	Pobe	6.93	2.67	1924	Badoplu
9	Bembereke	10.2	2.67	1921	Badoplu	37	Porto	6.48	2.62	1900	Badoplu
10	Beterou	9.2	2.27	1954	Badoplu	38	Sakete	6.72	2.67	1921	Badoplu
11	Bohicon	7.2	2.06	1940	Badoplu	39	Savalou	7.93	1.96	1921	Badoplu
12	Bopa	6.57	1.97	1922	Badoplu	40	Save	8.02	2.48	1921	Badoplu
13	Aéroport	6.35	2.38	1953	Badoplu	41	Tanguieta	10.62	1.27	1937	Badoplu
14	Cotonou	6.35	2.43	1922	Badoplu	42	Toffo	6.83	2.05	1953	Badoplu
15	Dassa	7.75	2.17	1941	Badoplu	43	Toui	8.68	2.59	1944	Badoplu
16	Dogbo	6.75	1.78	1953	Badoplu	44	Zagnanado	7.25	2.33	1921	Badoplu

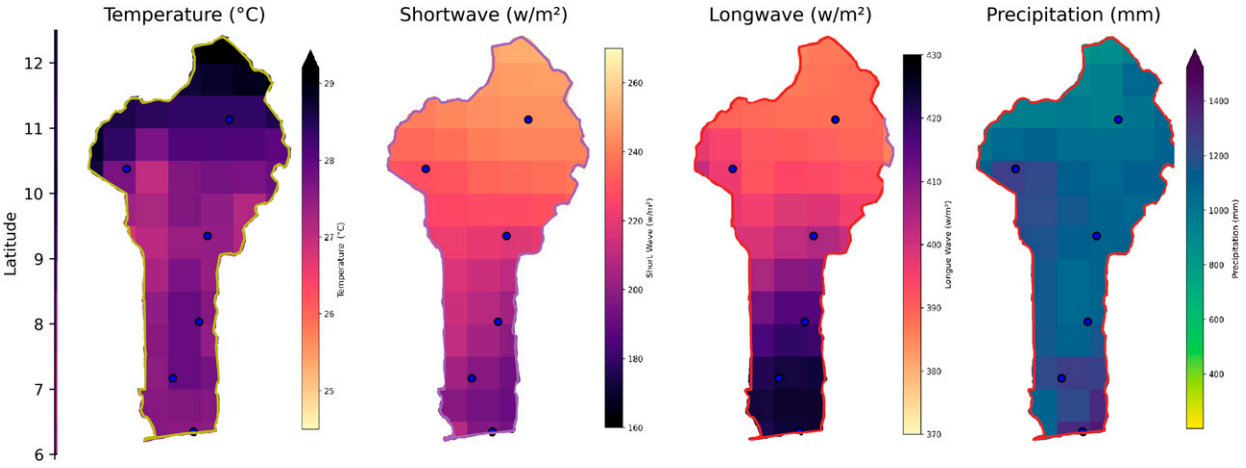

FIG. A1. Spatial distribution of WFDE5 reanalyzed for the average (left) temperature, (left center) SW, (right center) LW, and (right) precipitation.

REFERENCES

Amoussou, E., and Coauthors, 2016: Évolution climatique du Bénin de 1950 à 2010 et son influence sur les eaux de surface. *Colloque de l'Association Internationale de Climatologie: Climat et Pollution de l'air*, Besançon, France, Association Internationale de Climatologie, 231–236, https://hal.science/hal-01360108.

Atedhor, G. O., P. A. O. Odjugo, and A. E. Uriri, 2011: Changing rainfall and anthropogenic-induced flooding: Impacts and adaptation strategies in Benin City, Nigeria. *J. Geogr. Reg. Plan.*, **4**, 42–52.

Awange, J. L., V. G. Ferreira, E. Forootan-Khandu, S. A. Andam-Akorful, N. O. Agutu, and X. F. He, 2016: Uncertainties in remotely sensed precipitation data over Africa. *Int. J. Climatol.*, **36**, 303–323, https://doi.org/10.1002/joc.4346.

Babić, K., N. Kalthoff, B. Adler, J. F. Quinting, F. Lohou, C. Dione, and M. Lothon, 2019: What controls the formation of nocturnal low-level stratus clouds over southern West Africa during the monsoon season? *Atmos. Chem. Phys.*, **19**, 13 489–13 506, https://doi.org/10.5194/acp-19-13489-2019.

Badameli, A., and V. Dubreuil, 2015: Diagnostic du changement climatique au Togo à travers l'évolution de la température entre 1961 et 2010. *XXVIIIe Colloque de l'Association Internationale de Climatologie*, Liège, Belgium, Association Internationale de Climatologie, 421–426, http://www.climato.be/aic/colloques/actes/ACTES_AIC2015/5%20Variabilites%20et%20aleas%20climatiques/067-BADAMELI-421-426.pdf.

Bárdossy, A., and G. Pegram, 2013: Interpolation of precipitation under topographic influence at different time scales. *Water Resour. Res.*, **49**, 4545–4565, https://doi.org/10.1002/wrcr.20307.

Bodjrènou, R., L. O. Sintondji, and F. Comandan, 2023a: Hydrological modeling with physics-based models in the Oueme basin: Issues and perspectives for simulation optimization. *J. Hydrol. Reg. Stud.*, **48**, 101448, https://doi.org/10.1016/j.ejrh.2023.101448.

——, F. Comandan, and D. K. Danso, 2023b: Assessment of current and future land use and land cover in the Oueme basin for hydrological studies. *Sustainability*, **15**, 2245, https://doi.org/10.3390/su15032245.

Clark, M. P., D. E. Rupp, R. A. Woods, H. J. Tromp-van Meerveld, N. E. Peters, and J. E. Freer, 2009: Consistency between hydrological models and field observations: Linking processes at the hillslope scale to hydrological responses at the watershed scale. *Hydrol. Processes*, **23**, 311–319, https://doi.org/10.1002/hyp.7154.

Cucchi, M., G. P. Weedon, A. Amici, N. Bellouin, S. Lange, H. Müller Schmied, H. Hersbach, and C. Buontempo, 2020: WFDE5: Bias-adjusted ERA5 reanalysis data for impact studies. *Earth Syst. Sci. Data*, **12**, 2097–2120, https://doi.org/10.5194/essd-12-2097-2020.

Danso, D. K., S. Anquetin, A. Diedhiou, C. Lavaysse, A. Kobea, and N. E. Touré, 2019: Spatio-temporal variability of cloud cover types in West Africa with satellite-based and reanalysis data. *Quart. J. Roy. Meteor. Soc.*, **145**, 3715–3731, https://doi.org/10.1002/qj.3651.

——, ——, ——, and A. Adamou, 2020a: Cloudiness information services for solar energy management in West Africa. *Atmosphere*, **11**, 857, https://doi.org/10.3390/atmos11080857.

——, ——, ——, K. Kouadio, and A. T. Kobea, 2020b: Daytime low-level clouds in West Africa—Occurrence, associated drivers, and shortwave radiation attenuation. *Earth Syst. Dyn.*, **11**, 1133–1152, https://doi.org/10.5194/esd-11-1133-2020.

De Longueville, F., Y.-C. Hountondji, I. Kindo, F. Gemenne, and P. Ozer, 2016: Long-term analysis of rainfall and temperature data in Burkina Faso (1950–2013). *Int. J. Climatol.*, **36**, 4393–4405, https://doi.org/10.1002/joc.4640.

Dembélé, M., B. Schaefli, N. van de Giesen, and G. Mariéthoz, 2020: Suitability of 17 gridded rainfall and temperature datasets for large-scale hydrological modelling in West Africa. *Hydrol. Earth Syst. Sci.*, **24**, 5379–5406, https://doi.org/10.5194/hess-24-5379-2020.

Ebert, E. E., J. E. Janowiak, and C. Kidd, 2007: Comparison of near-real-time precipitation estimates from satellite observations and numerical models. *Bull. Amer. Meteor. Soc.*, **88**, 47–64, https://doi.org/10.1175/BAMS-88-1-47.

Fan, H., and D. He, 2015: Temperature and precipitation variability and its effects on streamflow in the upstream regions of the Gancang–Mekong and Nu–Salween Rivers. *J. Hydrometeor.*, **16**, 2248–2263, https://doi.org/10.1175/JHM-D-14-0238.1.

Fink, A., H. Paeth, V. Ermert, S. Pohle, and M. Diederich, 2010: Meteorological processes influencing the weather and climate of Benin. *Impacts of Global Change on the Hydrological Cycle in West and Northwest Africa*, P. Speth, M. Christoph, and B. Diekkrüger, Eds., Springer, 135–149.

Galle, S., and Coauthors, 2018: AMMA-CATCH, a critical zone observatory in West Africa monitoring a region in transition. *Vadose Zone J.*, **17**, 180062, https://doi.org/10.2136/vzj2018.03.0062.

Gelaro, R., and Coauthors, 2017: The Modern-Era Retrospective Analysis for Research and Applications, version 2 (MERRA-2). *J. Climate*, **30**, 5419–5454, https://doi.org/10.1175/JCLI-D-16-0758.1.

Gleixner, S., T. Demissie, and G. T. Diro, 2020: Did ERA5 improve temperature and precipitation reanalysis over East Africa? *Atmosphere*, **11**, 996, https://doi.org/10.3390/atmos11090996.

Grenier, P., C. Mailloux, É. Akpinfa, M. N. Agbazo, D. Chaumont, and Y. Rousseau, 2020: Atlas climatique du Bénin. Ouranos and Oxfam, 159 pp.

Gupta, D., and C. T. Maravelias, 2019: Online scheduling: Understanding the impact of uncertainty. *IFAC-PapersOnLine*, **52**, 727–732, https://doi.org/10.1016/j.ifacol.2019.06.149.

Gupta, H. V., H. Kling, K. K. Yilmaz, and F. M. Guillermo, 2009: Decomposition of the mean squared error and NSE performance criteria: Implications for improving hydrological modelling. *J. Hydrol.*, **377**, 80–91, https://doi.org/10.1016/j.jhydrol.2009.08.003.

Hersbach, H., and Coauthors, 2020: The ERA5 global reanalysis. *Quart. J. Roy. Meteor. Soc.*, **146**, 1999–2049, https://doi.org/10.1002/qj.3803.

Knippertz, P., and Coauthors, 2015: The DACCIWA project: Dynamics–Aerosol–Chemistry–Cloud Interactions in West Africa. *Bull. Amer. Meteor. Soc.*, **96**, 1451–1460, https://doi.org/10.1175/BAMS-D-14-00108.1.

Knoben, W. J. M., J. E. Freer, and R. A. Woods, 2019: Technical note: Inherent benchmark or not? Comparing Nash–Sutcliffe and Kling–Gupta efficiency scores. *Hydrol. Earth Syst. Sci.*, **23**, 4323–4331, https://doi.org/10.5194/hess-23-4323-2019.

Kollet, S. J., and R. M. Maxwell, 2005: Integrated surface-groundwater flow modeling: A free-surface overland flow boundary condition in a parallel groundwater flow model. *Adv. Water Resour.*, **29**, 945–958, https://doi.org/10.1016/j.advwatres.2005.08.006.

Lawin, A. E., N. R. Hounguè, C. A. Biaou, and D. F. Badou, 2019: Statistical analysis of recent and future rainfall and temperature variability in the Mono River watershed (Benin, Togo). *Climate*, **7**, 8, https://doi.org/10.3390/cli7010008.

Le Barbé, L., G. Alé, B. Millet, H. Texier, Y. Borel, and R. Gualde, 1993: *Les Ressources en Eaux Superficielles de la République du Bénin*. ORSTOM, 543 pp.

Ledesma, J. L. J., and M. N. Futter, 2017: Gridded climate data products are an alternative to instrumental measurements as inputs to rainfall–runoff models. *Hydrol. Processes*, **31**, 3283–3293, https://doi.org/10.1002/hyp.11269.

Lin, B., and B. Xu, 2018: Growth of industrial CO_2 emissions in Shanghai City: Evidence from a dynamic vector autoregression analysis. *Energy*, **151**, 167–177, https://doi.org/10.1016/j.energy.2018.03.052.

Loua, R. T., H. Bencherif, N. Mbatha, N. Bègue, A. Hauchecorne, Z. Bamba, and V. Sivakumar, 2019: Study on temporal variations of surface temperature and rainfall at Conakry Airport, Guinea: 1960–2016. *Climate*, **7**, 93, https://doi.org/10.3390/cli7070093.

Ly, S., C. Charles, and A. Degré, 2013: Different methods for spatial interpolation of rainfall data for operational hydrology and hydrological modeling at watershed scale: A review. *Biotech. Agron. Soc. Environ.*, **17**, 392–406, https://doi.org/10.6084/M9.FIGSHARE.1225842.V1.

Maidment, R. I., D. I. F. Grimes, R. P. Allan, H. Greatrex, O. Rojas, and O. Leo, 2013: Evaluation of satellite-based and model re-analysis rainfall estimates for Uganda. *Meteor. Appl.*, **20**, 308–317, https://doi.org/10.1002/met.1283.

Muñoz-Sabater, J., 2019: ERA5-land hourly data from 1981 to present. Copernicus Climate Change Service Climate Data Store, accessed 25 January 2021, https://doi.org/10.24381/Cds.E2161bac.

Neher, I., S. Crewell, S. Meilinger, U. Pfeifroth, and J. Trentmann, 2020: Long-term variability of solar irradiance and its implications for photovoltaic power in West Africa. *EGU General Assembly*, Online, EGU2020-19283, https://doi.org/10.5194/egusphere-egu2020-19283.

Nkrumah, F., T. Vischel, G. Panthou, N. A. B. Klutse, D. C. Adukpo, and A. Diedhiou, 2019: Recent trends in the daily rainfall regime in southern West Africa. *Atmosphere*, **10**, 741, https://doi.org/10.3390/atmos10120741.

N'Tcha M'Po, Y., 2016: Comparison of daily precipitation bias correction methods based on four regional climate model outputs in Ouémé basin, Benin. *Hydrology*, **4**, 58–71, https://doi.org/10.11648/j.hyd.20160406.11.

Ocio, D., T. Beskeen, and K. Smart, 2019: Fully distributed hydrological modelling for catchment-wide hydrological data verification. *Hydrol. Res.*, **50**, 1520–1534, https://doi.org/10.2166/nh.2019.006.

Oguntunde, P. G., B. J. Abiodun, and G. Lischeid, 2012: Spatial and temporal temperature trends in Nigeria, 1901–2000. *Meteor. Atmos. Phys.*, **118**, 95–105, https://doi.org/10.1007/s00703-012-0199-3.

Patchali, T. E., O. Ajide, O. J. Matthew, T. A. O. Salau, and O. M. Oyewola, 2020: Examination of potential impacts of future climate change on solar radiation in Togo, West Africa. *SN Appl. Sci.*, **2**, 1941, https://doi.org/10.1007/s42452-020-03738-3.

Peugeot, C., and Coauthors, 2011: Mesoscale water cycle within the West African monsoon. *Atmos. Sci. Lett.*, **12**, 45–50, https://doi.org/10.1002/asl.309.

Probst, E., and W. Mauser, 2022: Regional studies evaluation of ERA5 and WFDE5 forcing data for hydrological modelling and the impact of bias correction with regional climatologies: A case study in the Danube River basin. *J. Hydrol. Reg. Stud.*, **40**, 101023, https://doi.org/10.1016/j.ejrh.2022.101023.

Quagraine, K. A., F. Nkrumah, C. Klein, N. A. B. Klutse, and K. T. Quagraine, 2020: West African summer monsoon precipitation variability as represented by reanalysis datasets. *Climate*, **8**, 111, https://doi.org/10.3390/cli8100111.

Satgé, F., D. Defrance, B. Sultan, M.-P. Bonnet, F. Seyler, N. Rouché, F. Pierron, and J.-E. Paturel, 2020: Evaluation of 23 gridded precipitation datasets across West Africa. *J. Hydrol.*, **581**, 124412, https://doi.org/10.1016/j.jhydrol.2019.124412.

Tapsoba, D., M. Haché, L. Perreault, and B. Bobée, 2004: Bayesian rainfall variability analysis in West Africa along cross sections in space–time grid boxes. *J. Climate*, **17**, 1069–1082, https://doi.org/10.1175/1520-0442(2004)017<1069:BRVAIW>2.0.CO;2.

Thiemig, V., M. Rojas, M. Zambrano-Bigiarini, and A. De Roo, 2013: Hydrological evaluation of satellite-based rainfall estimates over the Volta and Baro-Akobo Basin. *J. Hydrol.*, **499**, 324–338, https://doi.org/10.1016/j.jhydrol.2013.07.012.

Vose, R. S., D. R. Easterling, and B. Gleason, 2005: Maximum and minimum temperature trends for the globe: An update through 2004. *Geophys. Res. Lett.*, **32**, L23822, https://doi.org/10.1029/2005GL024379.